

# OSKR/OKAI: Systematic Optimization of Key Encapsulation Mechanisms from Module Lattice

Shiyu Shen<sup>1</sup>, Feng He<sup>1</sup>, Zhichuang Liang<sup>1</sup>, Yang Wang<sup>2</sup>, and Yunlei Zhao<sup>1(✉)</sup>

<sup>1</sup> School of Computer Science, Fudan University, China.

{syshe19,fhe20,zcliang19,ylzhao}@fudan.edu.cn

<sup>2</sup> School of Mathematics, Shandong University, China.

wyang1114@email.sdu.edu.cn

**Abstract.** In this work, we make *systematic* optimizations of key encapsulation mechanisms (KEM) based on module learning-with-errors (MLWE), covering algorithmic design, fundamental operation of number-theoretic transform (NTT), approaches to expanding encapsulated key size, and optimized implementation coding. We focus on Kyber (now in the Round-3 finalist of NIST PQC standardization) and Aegis (a variant of Kyber proposed at PKC 2020).

By careful analysis, we first observe that the algorithmic design of Kyber and Aegis can be optimized by the mechanism of asymmetric key consensus with noise (AKCN) proposed in [12,13]. Specifically, the decryption process can be simplified with AKCN, leading to a both faster and less error-prone decryption process. Moreover, the AKCN-based optimized version has perfect compatibility with the deployment of Kyber/Aegis in reality, as they can run on the same parameters, the same public key, and the same encryption process.

We make a systematic study of the variants of NTT proposed in recent years for extending its applicability scope, make concrete analysis of their exact computational complexity, and in particular show their equivalence. We then present a new variant named hybrid-NTT (H-NTT), combining the advantages of existing NTT methods, and derive its optimality in computational complexity. The H-NTT technique not only has larger applicability scope but also allows for modular and unified implementation codes of NTT operations even with varying module dimensions.

We analyze and compare the different approaches to expand the size of key to be encapsulated (specifically, 512-bit key for dimension of 1024), and conclude with the most economic approach. To mitigate the compatibility issue in implementations we adopt the proposed H-NTT method.

Each of the above optimization techniques is of independent value, and we apply all of them to Kyber and Aegis, resulting in new protocol variants named OSKR and OKAI respectively. For all the new protocol variants proposed in this work, we provide both AVX2 and ARM Cortex-M4 implementations, and present the performance benchmarks. Through thorough implementation optimizations, our AVX2 implementation gains efficiency improvement by 17.39% compared to Kyber-512, by 11.31% to Kyber-768, and by 34.26% to Kyber-1024. Meanwhile, our work shows 53.96%, 25.00%, and 49.08% improvement in speed and 82.57% reduction in pre-computed root storage compared to Aegis. Also, to the best of our knowledge, our work is the first that presents ARM Cortex-M4 implementations for the variants of Aegis.

**Keywords:** post-quantum cryptography (PQC), lattice-based cryptography, key encapsulation mechanism (KEM), number theoretic transform (NTT), software optimization

## 1 Introduction

Most public-key cryptosystems currently in use, based on the hardness of solving (elliptic curve) discrete logarithm or factoring large integers, will be broken if large-scale quantum computers are ever built. These cryptosystems are used to implement digital signatures and key establishment, and play a crucial role in ensuring the confidentiality and authenticity on the Internet and other networks. The arrival of such quantum computers is now believed by many scientists to be merely a significant engineering challenge. It is estimated to be within the next two decades. Due to this concern, post-quantum cryptography (PQC) was intensively investigated in recent years, and lattice-based cryptography is considered a prime candidate.

The requirement of security drove NIST to launch the PQC standardization competition in 2016. Recently, NIST announced seven finalist algorithms for the Round-3 competition, in which five algorithms are based on lattices with algebraic structures [22]. Among the various post-quantum proposals, Kyber [3], a mechanism based on the MLWE problem, represents one of the most promising KEM schemes constructed on module lattice. The design rationale goes back to the first LWE-based encryption scheme presented by Regev [23], with the elements of vectors changing from integers to polynomials. Recently, Zhang et al. [28] present a variant of Kyber, named Aigis, based on the the asymmetric version of MLWE. These two algorithms share the same encryption/decryption mechanism, and the difference lies in the details: (1) Kyber eliminates public-key compression since its Round-2 submission, while Aigis retains it. Actually, Aigis can be viewed as the Round-1 version of Kyber but with the secret and noise parameters changed; (2) Aigis-1024 encapsulates a 512-bit key, in which  $q$  is changed from 7681 (for the dimensions of 512 and 768) to 12289 for the dimension of 1024. Kyber keep encapsulating 256-bit shared key with unified  $q = 3329$ .

For cryptographic algorithms based on lattices with algebraic structures like module lattices, one fundamental and time-consuming operation is the multiplication of the elements in the polynomial quotient ring  $\mathbb{Z}_q[x]/(\Phi(x))$ , where  $q$  is a prime and  $\Phi(x)$  is a cyclotomic polynomial of degree  $n$  [20]. Typically,  $\Phi(x) = x^n + 1$  where  $n$  is a power of 2. There are two main approaches to fast polynomial multiplications in this setting: the number theoretic transform (NTT) [7,9], and the Toom-Cook and Karatsuba based methods [8,15,26]. Generally speaking, NTT is the most efficient multiplication over rings, due to its quasilinear  $O(n \log n)$  time complexity. Nevertheless, the traditional NTT technique puts some restrictions on the modulus and dimension of the underlying ring, and has two major problems in applications. Specifically, it requires  $2n|(q - 1)$  and  $n$  be a power of two. Along with the progress of NIST PQC standardization, many research efforts have been made in recent years for generalizing the NTT technique. To relax the requirement on  $2n|(q - 1)$ , the work [29] proposed the “upper dividing” approach referred to as *preprocess-then-NTT* (Pt-NTT), and the work of Kyber [3] proposed the “bottom cropping” approach that is referred to as *truncated-NTT* (T-NTT) in this work for presentation simplicity. The upper dividing (resp., bottom cropping) method was further improved in [30] (resp., [1]) by combining it with the Karatsuba technique [27]. The Karatsuba technique can reduce the number of multiplications at the cost of additional additions. To our knowledge, the relationship between Pt-NTT [29,30] and T-NTT [1,3] was not explicitly studied in the literature. Also, the analysis of the exact computational complexity of Pt-NTT and T-NTT is inadequate or incomplete in the literature.

In the post-quantum era, 256-bit keys are not enough for SKC (symmetric-key cryptography) aimed at 256-bit pq-security. In this case, we have to encapsulate larger keys for SKC of 256-bit pq-sec. For Kyber, the keys encapsulated for all three sets of parameters have the fixed size of 256 bits, while for Aigis-1024 the key size is set to be 512 bits. Here, we discuss the desirability of larger key size.

- Doubling the key size means more powerful and economic ability of key transportation, at about the same level of security and bandwidth.
- For some application scenarios demanding critical security guarantees, symmetric-key cryptographic primitives of larger key size (particularly, key size of 512 bits) are already in use in practice.
- Fixing key size for different security levels is less flexible. A more flexible and desirable way is to allow users to negotiate the key sizes according to different security levels and application scenarios. For example, according to different security levels (specifically, 128, 192, 256-bit classic security), in TLS 1.3 [24] it mandates three options for the master secrecy size: 256, 384 and 512, by negotiating and employing the secp256r1, secp384r1 and secp512r1 curves respectively.
- Doubling the shared-key size is important for the targeted security level against Grover’s search algorithm, and against the possibility of more sophisticated quantum cryptanalysis in the long run. Note that for Kyber-1024, its target security level is about 230-bit post-quantum security (pq-security). Even if the underlying lattice hard problems provide this level of hardness, the 256-bit shared-key may not. For example, the updated quantum analysis on AES [11] overall reduces the original estimate of quantum cost in bits against AES (specified in the call for proposals of NIST PQC standardization [21]) between 11 and 13, and this line of research is quite active now. Though the standardization of post-quantum symmetric key cryptography is not considered yet, it is expected that the key size will increase to remain at the same security level in the post-quantum era.

As we shall show, there can be three different approaches to achieving the goal of encapsulating larger keys. But these approaches were not analyzed and measured quantitatively.

## 1.1 Our Contributions

In this work, we make *systematic* optimizations of key encapsulation mechanisms (KEM) based on module learning-with-errors (MLWE), covering algorithmic design, fundamental operation of number-theoretic transform (NTT), approaches to expanding encapsulated key size, and optimized implementation coding. Our contributions can be summarized as below:

1. **AKCN-based faster and less error-prone decryption.** By extracting the underlying mathematical structure behind the algorithmic design and by careful probability analysis, we observe that the decryption process of Kyber/Aigis can be optimized by the mechanism of asymmetric key consensus with noise (AKCN) proposed by Jin and Zhao in [12,13], leading to a both faster and less error-prone decryption process. Moreover, the AKCN-based optimized version with this technique has perfect compatibility with the deployment of Kyber/Aigis in reality, as they can run on the same parameters, the same public key, and the same encryption process, except the decryption process is simplified to be faster and less error-prone.
2. **Hybrid number theoretic transformation.** We make a systematic study of the NTT technique. More specifically, let  $\alpha$  and  $\beta$  be nonnegative integers, Pt-NTT [29,30] follows the upper dividing approach, where  $\alpha$  levels of 2-division are made from the top. On the contrary, T-NTT follows the bottom cropping approach, where  $\beta$  levels are cropped from the bottom. These two approaches appear to be quite different. However, the truth is that they are computationally equivalent, as we shall show in this work. Based on this, we combine the upper dividing approach and the bottom cropping approach, and applying the Karatsuba technique all together, and propose a new variant of NTT referred to as *hybrid number theoretic transform* (H-NTT for short). In particular, Pt-NTT and T-NTT can be viewed as the special cases of H-NTT. We make a complete and comprehensive analysis of the exact computational complexity of H-NTT, and derive its optimal bound with respect to any fixed parameters of  $(n, q)$ . The H-NTT technique is more flexible, which not only has larger applicability scope but also allows for modular and unified implementation codes of NTT operations even with varying module dimensions.
3. **Expansion to 512-bit shared key.** We analyze and compare the different approaches to expand the size of key to be encapsulated (specifically, 512-bit key for dimension of 1024). There are three ways to encapsulate a 512-bit key: (1) encapsulating twice and combining them; (2) changing the encoding method of message from one bit to two bits; (3) changing the dimension from 256 to 512. In this work, we make a detailed analysis and comparison of these methods in respect of bandwidth, decryption error probability, and security. We conclude that the third approach is the most economic way, but it suffers from relatively poor compatibility. That is also the reason that Aigis uses a different modulus  $q = 12289$  for this case. However, once we combine it with our H-NTT technique, this problem can be well handled. Finally, we instantiate the three approaches with the parameters derived from Kyber [3,2], and the results confirm the findings of our research.
4. **Applications to Kyber and Aigis.** Each of the above optimization techniques is of independent value, and we apply all of them to Kyber and Aigis. For applications to Kyber, we optimize its decryption process to be faster and less error-prone, and also present a new parameter set for Kyber-1024 with our H-NTT technique for encapsulating 512-bit key. The resultant scheme is named OSKR (standing for Optimized and Security-strengthened Kyber). The H-NTT based implementation of OSKR-1024 can re-use the T-NTT codes for OSKR-512 and OSKR-768. In other words, though the parameter set for OSKR-1024 is changed from Kyber-1024, there is no need for modifying the codes of NTT in implementation. For applications to Aigis, we present a new variant of it, referred to as OKAI (standing for Optimized KEM from Aigis). As with OSKR, we optimize its decryption to be faster and less error-prone. More importantly, we unify the parameters for all the three sets of OKAI-512, 768 and 1024, by setting the same  $q = 7681$  and the same secret and noise distribution parameters. We apply T-NTT (with  $\beta = 1$ ) and H-NTT (with  $\alpha = \beta = 1$ ) respectively for implementing OKAI-512/768 and OKAI-1024 respectively. The

unified parameters and the T-NTT technique allow for more modular and space-efficient implementations. OKAI-768 and Aegis-768 (that is the recommended version of Aegis) share the same set of parameters. For the dimension of 1024, compared to Aegis-1024, at about the same level of security OKAI-1024 enjoys smaller bandwidth, lower error probability, and faster decryption simultaneously.

5. **Optimized implementation.** For all the new protocol variants proposed in this work, we make comprehensive implementations and thorough coding optimizations. We provide both AVX2 and ARM Cortex-M4 implementations, and present the performance benchmarks. Through thorough implementation optimizations, our AVX2 implementation gains efficiency improvement by 17.39% compared to Kyber-512, by 11.31% to Kyber-768, and by 34.26% to Kyber-1024. Meanwhile, our work shows 53.96%, 25.00%, and 49.08% improvement in speed and 82.57% reduction in pre-computed roots storage compared to Aegis. Also, to the best of our knowledge, our work is the first that presents ARM Cortex-M4 implementations for the variants of Aegis.

**Table 1.** Comparisons among Kyber, Aegis, and our schemes

Schemes	$n$	$q$	$\delta$	$pq - sec$	$ pk $	$ ct $	$ K $	Cycles	Speedup
Kyber	512	3329	$2^{-138.9}$	100	800	768	32	986698	-
	768	3329	$2^{-165}$	164	1184	1088	32	1569400	
	1024	3329	$2^{-174.9}$	230	1568	1568	32	2528844	
OSKR	512	3329	<b><math>2^{-142.8}</math></b>	100	800	768	32	815120	<b>17.39%</b>
	768	3329	<b><math>2^{-168.8}</math></b>	164	1184	1088	32	1391824	<b>11.31%</b>
	1024	3329	<b><math>2^{-178.7}</math></b>	230	1600	1728	<b>64</b>	1662440	<b>34.26%</b>
Aegis	512	7681	$2^{-81.9}$	100	672	672	32	2064849	-
	768	7681	$2^{-128.7}$	147	896	992	32	2316184	
	1024	12289	$2^{-211.8}$	213	1472	1536	64	3815884	
OKAI	512	7681	<b><math>2^{-85.3}</math></b>	90	<b>608</b>	<b>640</b>	32	950616	<b>53.96%</b>
	768	7681	<b><math>2^{-132.7}</math></b>	147	896	992	32	1737024	<b>25.00%</b>
	1024	<b>7681</b>	<b><math>2^{-216.2}</math></b>	208	<b>1344</b>	<b>1472</b>	64	1942956	<b>49.08%</b>

## 2 Preliminaries

### 2.1 Notation

Let  $n$  be a positive integer, especially a power of 2, and  $q$  be a prime number. Then  $\mathbb{Z}_q$  denotes the quotient ring  $\mathbb{Z}/q\mathbb{Z}$ . Let  $\mathcal{R} = \mathbb{Z}[X]/(\Phi(X))$  be the ring of integer polynomials modulo  $\Phi(X)$ , where  $\Phi(X)$  is the cyclotomic polynomial of degree  $n$ . Define  $\mathcal{R}_q = \mathcal{R}/q\mathcal{R} = \mathbb{Z}_q[X]/(\Phi(X))$ . It indicates each polynomial in  $\mathcal{R}_q$  comes from  $\mathcal{R}$  and the coefficients are in  $\mathbb{Z}_q$ .  $\mathcal{B}$  denotes the string space. By default, regular font letters denote elements in  $\mathcal{R}$  or  $\mathcal{R}_q$ , bold lower-case letters are vectors and bold upper-case letters are matrices. Denote  $\mathbf{a}^T$  as the transpose of a vector  $\mathbf{a}$ , and the same for a matrix.

*Polynomials* A polynomial in  $\mathcal{R}_q$ , denoted as  $f$ , can be represented as  $f = \sum_{i=0}^{n-1} f_i X^i$ . The column vector form of  $f$  is  $f = (f_0, f_1, \dots, f_{n-1})^T$ , and the row vector form is  $f = (f_0, f_1, \dots, f_{n-1})$ , where  $f_i \in \mathbb{Z}_q, i = 0, 1, \dots, n-1$ .

*Operations* For an element  $x \in \mathbb{Q}$ , we denote by  $\lceil x \rceil$  rounding of  $x$  to the closest integer. For a set  $S$ , let  $s \leftarrow S$  mean that  $s$  is chosen uniformly at random from  $S$ . Let  $|\cdot|$  be the length of a string in bytes or the absolute value of a number. Denote  $\text{mod}^{\pm} q$  the modular reduction operation that reduce an even (resp., odd) positive integer to the range  $(-\frac{q}{2}, \frac{q}{2}]$  (resp.,  $[-\frac{q-1}{2}, \frac{q-1}{2}]$ ). For an element  $a \in \mathbb{Z}_q$ , we write  $\|a\|_{\infty}^{\pm}$  to mean  $|a \text{ mod } \pm q|$ . For a polynomial  $a = \sum_{i=0}^{n-1} a_i X^i \in \mathcal{R}$ , we write  $\|a\|_{\infty}^{\pm} = \max_i \|a_i\|_{\infty}^{\pm}$ . For a vector  $\mathbf{a} = (a_0, \dots, a_{n-1})$ , define  $\|\mathbf{a}\|_{\infty}^{\pm} = \max_i \|a_i\|_{\infty}^{\pm}$ .

*Symbols* Denote  $\psi_\eta$  as the centered binomial distribution, which can be computed with  $\sum_{i=0}^\eta (a_i - b_i)$  where the bits  $a_i$  and  $b_i$  are chosen uniformly at random from  $\{0, 1\}$ . For the scheme's parameters, denote by  $n$  the dimension of the underlying module polynomial,  $q$  the prime modulus,  $l$  the dimension of the vector, and  $\log m$  the number of bits to be encoded via each dimension. In addition, we use  $\eta$  to indicate the size of the noise, and  $d$  (resp.,  $t$ ) to indicate the number of bits which an integer in  $\mathbb{Z}_q$  is compressed into (resp., cut out), and set  $g = 2^d$ . The subscripts are related to variables, for example,  $\eta_s$  indicates that the coefficients of polynomial  $s$  are in the interval  $[-\eta_s, \eta_s]$ . And the superscript indicates the dimension of the vector. Denote by  $pk$  the public key,  $sk$  the secret key,  $ct$  the ciphertext, and  $B$  the communication bandwidth that is the sum of the lengths of the public key and the ciphertext. The metric used here is byte. When analyzing the schemes, let  $\delta$  be the error probability of decryption,  $pq\text{-sec}$  be the post-quantum security level in bits, and  $K$  be the key to be encapsulated.

## 2.2 Karatsuba technique

**Definition 1 (Karatsuba technique[27]).** Let  $a, b, c$  and  $d$  be four numbers. To compute  $s = a \cdot c + b \cdot d$ , the Karatsuba technique uses the previously calculated  $s_1 = a \cdot b$  and  $s_2 = c \cdot d$ , and computes  $s = (a + b) \cdot (c + d) - s_1 - s_2$ .

Since the two previously calculated values are reused, this method is equivalent to replacing one multiplication with three additions or subtractions. The computational platform determines the exact effect. If the overhead of multiplication is high on a target platform, then good results can be achieved using this method.

## 2.3 Number Theoretic Transform

The Number Theoretic Transform (NTT) is a special version of a Fast Fourier Transform (FFT) over a finite field. Let  $\mathcal{R}_q = \mathbb{Z}_q[x]/(x^n + 1)$ , where  $n$  is a power of 2 and  $q$  is a prime satisfying  $2n|(q - 1)$ . According to the traditional  $n$ -length NTT approach, to compute  $h = fg \in \mathcal{R}_q$ , where  $f, g \in \mathcal{R}_q$ , we first let  $\tilde{f} = (1, \omega, \omega^2, \dots, \omega^{n-1}) \circ f$ ,  $\tilde{g} = (1, \omega, \omega^2, \dots, \omega^{n-1}) \circ g$ . Here “ $\circ$ ” denotes the pointwise multiplication of vectors and  $\omega$  is the  $2n$ -th primary root of unity in  $\mathbb{Z}_q$ . Define the forward transformation  $\hat{f} = NTT(\tilde{f})$  as  $\hat{f}_j = \sum_{i=0}^{n-1} \tilde{f}_i \gamma^{ij} \bmod q$ , and the inverse transformation  $\tilde{f} = NTT^{-1}(\hat{f})$  as  $\tilde{f}_i = n^{-1} \sum_{j=0}^{n-1} \hat{f}_j \gamma^{-ij} \bmod q$ , where  $i, j = 0, 1, \dots, n - 1$  and  $\gamma = \omega^2 \bmod q$ . Then, we compute  $\tilde{h} = NTT^{-1}(NTT(\tilde{f}) \circ NTT(\tilde{g}))$ , and get  $h = (1, \omega^{-1}, \omega^{-2}, \dots, \omega^{-(n-1)}) \circ \tilde{h}$ .

Let  $\widehat{NTT}(f) = NTT((1, \omega, \omega^2, \dots, \omega^{n-1}) \circ f)$ , and  $\widehat{NTT}^{-1}(\hat{f}) = (1, \omega^{-1}, \omega^{-2}, \dots, \omega^{-(n-1)}) \circ NTT^{-1}(\hat{f})$ . The above equation can be transformed into  $h = \widehat{NTT}^{-1}(\widehat{NTT}(f) \circ \widehat{NTT}(g))$ . By analyzing this process, we can get that in the forward NTT, the computational complexity of multiplication is  $T_m(\widehat{NTT}) = \frac{1}{2}n \log n$  and the computational complexity of addition is  $T_a(\widehat{NTT}) = n \log n$ . In the inverse NTT, these two are  $T_m(\widehat{NTT}^{-1}) = \frac{1}{2}n \log n + n$  and  $T_a(\widehat{NTT}^{-1}) = n \log n$ , respectively.

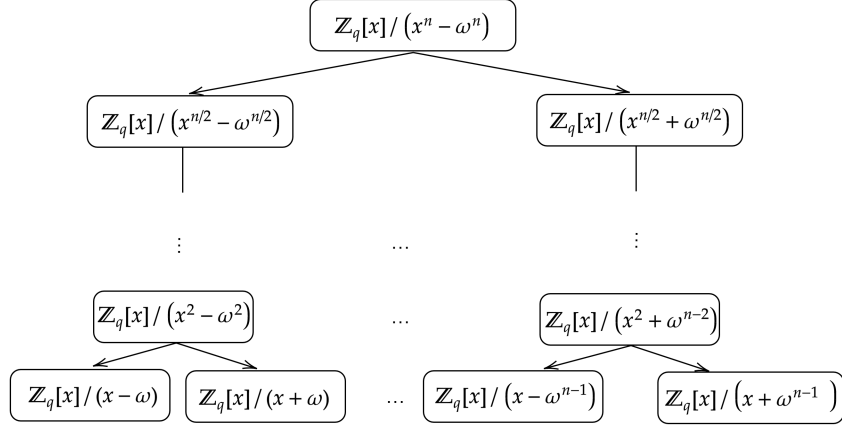


**Fig. 1.** Tree decomposition of NTT calculation process

The calculation process is shown in Figure 1. This is a decomposition of the ring, which is reflected in the following decomposition of the Chinese remainder theorem (CRT). Thus, we only demand the images of  $f$  and  $g$  in  $\mathbb{Z}_q[x]/(x - \omega^i)$ , where  $i \in \{1, 3, \dots, 2n - 1\}$ . In the proof that follows, we use the matrix form for the sake of brevity of expression, as shown in Definition 2.

$$\mathbb{Z}_q[x]/(x^n + 1) \cong \mathbb{Z}_q[x]/(x - \omega) \times \dots \times \mathbb{Z}_q[x]/(x - \omega^{2n-1}). \quad (1)$$

**Definition 2.** Based on the explanation of NTT with CRT, we can think of the NTT process as a unique form of interpolation. Note that the process of the interpolation is a linear transformation, which can be represented in the matrix form:

$$\begin{bmatrix} \hat{f}_0 \\ \hat{f}_1 \\ \vdots \\ \hat{f}_{n-1} \end{bmatrix} = \begin{bmatrix} 1 & \omega & \omega^2 & \dots & \omega^{n-1} \\ 1 & \omega^3 & \omega^6 & \dots & \omega^{2n-2} \\ \vdots & \vdots & \vdots & \ddots & \vdots \\ 1 & \omega^{2n-1} & \omega^{4n-2} & \dots & \omega^{(2n-1)(n-1)} \end{bmatrix} \cdot \begin{bmatrix} f_0 \\ f_1 \\ \vdots \\ f_{n-1} \end{bmatrix} \quad (2)$$

where we denote the coefficient matrix above by  $\mathbf{W}_n$ .

## 2.4 Hard Problems on Lattice

The LWE problem [23] allows for a flexible choice of parameters, while the Ring-LWE (RLWE) problem [19] has stable structural properties. Based on this, [18] makes a trade-off between security and efficiency, and provides a combined version of the standard LWE problem and the RLWE problem, called the Module-LWE (MLWE) problem. Let  $\mathcal{R}$  and  $\mathcal{R}_q$  denote the rings  $\mathbb{Z}[x]/(x^n + 1)$  and  $\mathbb{Z}_q[x]/(x^n + 1)$ , respectively. Denote by  $S_\eta \subseteq \mathcal{R}^l$  the set of elements  $w \in \mathcal{R}^l$  such that  $\|w\|_\infty \leq \eta$ , where  $l \geq 0$  is an integer. Roughly speaking, the search version of the MLWE problem states that given  $\mathbf{A} \leftarrow \mathcal{R}_q^{l \times l}$  and  $\mathbf{b} := \mathbf{A}\mathbf{s} + \mathbf{e}$ , where  $\mathbf{s}, \mathbf{e} \leftarrow S_\eta$ , no efficient algorithm can recover  $\mathbf{s}$  with non-negligible probability. The decision version of the MLWE problem states that given samples  $(\mathbf{A}, \mathbf{b} := \mathbf{A}\mathbf{s} + \mathbf{e})$  where  $\mathbf{A} \leftarrow \mathcal{R}_q^{l \times l}$ ,  $\mathbf{s}, \mathbf{e} \leftarrow S_\eta$  and uniform samples  $(\mathbf{A}, \mathbf{b}) \leftarrow \mathcal{R}_q^{l \times l} \times \mathcal{R}_q^l$ , no efficient algorithm can distinguish them. Especially, when  $\mathbf{s}$  and  $\mathbf{e}$  are given from different distributions, the asymmetric version of the MLWE (AMLWE) problem can be provided. The AMLWE problem can be viewed as a special case of the MLWE problem with  $\mathbf{s} \leftarrow S_{\eta_s}$ ,  $\mathbf{e} \leftarrow S_{\eta_e}$  and  $\eta_s \neq \eta_e$ .

## 2.5 Polynomial Compression and Decompression

Some compression and decompression methods are often used in practice to save bandwidth and minimize the communication cost. Through this way, some low-order bits can be discarded in the public key and ciphertext, which do not have much effect on the correctness of the decryption. The most common functions and currently used in Kyber [3] and Aegis [28] are defined as:

$$\begin{cases} \text{Compress}_q(x, d) = \left\lfloor \frac{2^d}{q} x \right\rfloor \bmod 2^d \\ \text{Decompress}_q(y, d) = \left\lfloor \frac{q}{2^d} y \right\rfloor \bmod q, \end{cases} \quad (3)$$

Where  $d < \lceil \log_2(q) \rceil$ ,  $x \in \mathbb{Z}_q$  and  $y \in \mathbb{Z}_{2^d}$ . This **Compress** function takes an element  $x \in \mathbb{Z}_q$  and outputs an integer in  $\{0, \dots, 2^d - 1\}$ . Furthermore, by **Decompress** we get  $x' = \text{Decompress}_q(\text{Compress}_q(x, d), d)$  which satisfies the property [3] that

$$|x' - x \bmod \pm q| \leq B_q := \left\lceil \frac{q}{2^{d+1}} \right\rceil \quad (4)$$

Notice that there is one division operation in these functions, which is one of the most time-consuming operations in implementation. However, taking the method first proposed by Barrett [5], we can replace the division with one multiplication and one shift right operations; that is:

$$\left\lfloor \frac{a}{q} \right\rfloor = a \cdot b \gg s \quad (5)$$

where  $b = \left\lceil \frac{2^s}{q} \right\rceil$  and  $s > \log_2 aq$ . This method can improve computational efficiency, especially in parallel optimization, and it has recently been adopted in the Round-3 submission of Kyber [4].

## 3 Optimization of Decryption: Faster and Less Error-Prone

Note that Kyber and Aegis share the same public-key encryption mechanism, which is similar to the LPR encryption scheme introduced for Ring-LWE in [19] but based on Module-LWE instead of Ring-LWE and with polynomial compression. The basic CPA-secure suit consists of three parts, denoted as **CPAPKE** = (**KeyGen**, **Enc**, **Dec**). By extracting and studying the mathematical structure behind, we come to the conclusion that the two rounding operations in **CPAPKE.Dec** can be reduced to one. In this section, we give a concrete analysis, showing that the decryption procedure can be both more efficient and less error-prone with our new method.

### 3.1 AKCN-Based Optimization of the Decryption Function

Denote  $pk = (\mathbf{t}, \rho)$ ,  $sk = \mathbf{s}$ ,  $ct = (\mathbf{c}_1, c_2)$ ,  $r$  as the seed, and  $k$  as the secret polynomial to be encrypted,  $k_i \in \{0, 1\}$ . We recall the three algorithms of **CPAPKE** in Algorithm 1, 2 and 3, where functions **Parse**, **Sam** and **CBD** are used in uniform and binomial distribution sampling as defined in [2,3,4]. Note that the updated version of Kyber only compresses the ciphertext (for provable security reduced to MLWE), while Aegis follows the original structure of Kyber with public key and ciphertext both compressed.

After encryption, the information of  $k$  is hidden in  $c_2$  by decompressing and adding it to  $v$ . Let  $k_i, \sigma_{1,i}, \sigma_{2,i}$ , and  $k'_i$  be the  $i$ -th coefficient of  $k$ ,  $\sigma_1, \sigma_2$  and  $k', m = 2^{d_m}$ , and  $g = 2^{d_v}, i \in [0, n]$ . Focusing on each dimension of the polynomial, we have that the main encryption process of  $k_i$  in **Enc** and the decryption process of  $v_i$  in **Dec**, denoted **enc** and **dec** for presentation simplicity, have the following calculations:

$$v_i = \text{enc}(\sigma_{2,i}, k_i) = \left\lfloor \frac{g}{q} (\sigma_{2,i} + \left\lfloor \frac{q}{m} \right\rfloor \cdot k_i) \right\rfloor \bmod g \quad (6)$$

$$k'_i = \text{dec}(\sigma_{1,i}, v_i) = \left\lfloor \frac{m}{q} \left( \left\lfloor \frac{q}{g} \cdot v_i \right\rfloor - \sigma_{1,i} \right) \right\rfloor \bmod m \quad (7)$$

Specifically, `enc` (Algorithm 2, line 6) and `dec` (Algorithm 3, line 2) operate on every coefficient of the polynomials. In (6) the rounding of  $\frac{q}{2}$  can be pre-computed, so there remains only one rounding operation. However, the things are different in (7), where the two rounding operations may introduce more unexpected decryption errors. We observe it can be simplified as follows with only one rounding operation.

$$k'_i = \text{dec}(\sigma_{1,i}, v_i) = \left\lfloor m \left( \frac{v_i}{g} - \frac{\sigma_{1,i}}{q} \right) \right\rfloor \mod m \quad (8)$$

Where  $params = (q = 3329, m = 2, d_v \in \{4, 5\})$  in Kyber and  $params = (q \in \{7681, 12289\}, m = 2, d_v \in \{3, 4\})$  in Aegis.<sup>3</sup> We remark that the procedures of `enc` as specified in (6) and `dec` as specified in (8) just correspond to the procedures of `Con` and `Rec` respectively as specified in the AKCN mechanism [12,13].

---

**Algorithm 1** CPAPKE.KeyGen()

---

1: $\sigma, \rho \leftarrow \{0, 1\}^n$	▷ Generate $n$ -bit seeds $\sigma$ and $\rho$
2: $\mathbf{A} \leftarrow \mathbb{R}_q^{l \times l} := \text{Parse}(\text{Sam}(\rho))$	▷ Generate matrix $\mathbf{A}$
3: $(\mathbf{s}, \mathbf{e}) \leftarrow \psi_{\eta_s}^l \times \psi_{\eta_e}^l := \text{CBD}(\sigma)$	▷ Generate vectors $\mathbf{s}, \mathbf{e}$
4: $\mathbf{t} := \text{Compress}_q(\mathbf{As} + \mathbf{e}, d_t)$	▷ Calculate vector $\mathbf{t}$
5: <b>return</b> $(pk := (\mathbf{t}, \rho), sk := \mathbf{s})$	▷ Generate $pk$ and $sk$

---



---

**Algorithm 2** CPAPKE.Enc( $pk = (\mathbf{t}, \rho), k, r$ )

---

1: $\hat{\mathbf{t}} := \text{Decompress}_q(\mathbf{t}, d_t)$	▷ Decompress $\mathbf{t}$ to get $\hat{\mathbf{t}}$
2: $\hat{\mathbf{A}} \leftarrow \mathbb{R}_q^{l \times l} := \text{Parse}(\text{Sam}(\rho))$	▷ Generate matrix $\hat{\mathbf{A}}$
3: $(\mathbf{r}, \mathbf{e}_1, e_2) \leftarrow \psi_{\eta_s}^l \times \psi_{\eta_e}^l \times \psi_{\eta_e}^l := \text{CBD}(r)$	▷ Generate vectors $\mathbf{r}, \mathbf{e}_1$ and polynomial $e_2$
4: $\mathbf{u} := \text{Compress}_q(\hat{\mathbf{A}}^T \cdot \mathbf{r} + \mathbf{e}_1, d_u)$	▷ Calculate vector $\mathbf{u}$
5: $\sigma_2 := \hat{\mathbf{t}}^T \cdot \mathbf{r} + e_2$	▷ Calculate polynomial $\sigma_2$
6: $v := \text{Compress}_q(\sigma_2 + \text{Decompress}_q(k, d_m), d_v)$	▷ enc
7: <b>return</b> $ct := (\mathbf{c}_1 := \mathbf{u}, c_2 := v)$	

---



---

**Algorithm 3** CPAPKE.Dec( $sk = \mathbf{s}, ct = (\mathbf{c}_1 = \mathbf{u}, c_2 = v)$ )

---

1: $\sigma_1 = \mathbf{s}^T \cdot \text{Decompress}_q(\mathbf{u}, d_u)$	
2: $k' := \text{Compress}_q(\text{Decompress}_q(v, d_v) - \sigma_1, d_m)$	▷ dec
3: <b>return</b> $k'$	

---

### 3.2 Analysis of Error Probability

Define  $\mathbf{t}' = \mathbf{A} \cdot \mathbf{s} + \mathbf{e}$  in CPAPKE.KeyGen,  $\mathbf{u}' = \hat{\mathbf{A}}^T \cdot \mathbf{r} + \mathbf{e}_1$  and  $v' = \hat{\mathbf{t}}^T \cdot \mathbf{r} + e_2 + \lfloor \frac{q}{m} \rfloor \cdot k$  in CPAPKE.Enc. And define:

$$\begin{aligned} \varepsilon_1 &= \mathbf{t}' - \text{Decompress}_q(\text{Compress}_q(\mathbf{t}', d_u), d_u) \\ \varepsilon_2 &= \mathbf{u}' - \text{Decompress}_q(\text{Compress}_q(\mathbf{u}', d_u), d_u) \\ \varepsilon_v &= v' - \frac{q}{2^{d_v}} \left\lfloor \frac{2^{d_v}}{q} \cdot v' \right\rfloor \end{aligned}$$

<sup>3</sup> For (8), there can be many forms that can derive the shared secret. We only give an example which we believe to be more concise and precise.

The polynomial  $k'$  which contains the secret information that CPAPKE.Dec outputs is initially written as

$$\begin{aligned} k' &= \text{Compress}_q(v - \mathbf{s}^T \cdot \mathbf{u}, 1) \\ &= \left\lfloor \frac{m}{q} \left( \left\lfloor \frac{q}{2^{d_v}} \cdot c_2 \right\rfloor - \mathbf{s}^T \cdot \mathbf{u} \right) \right\rfloor \bmod m \end{aligned}$$

Omitting the rounding inside, we have

$$k' = \left\lfloor \frac{m}{q} \left( \frac{q}{2^{d_v}} \cdot c_2 - \mathbf{s}^T \cdot \mathbf{u} \right) \right\rfloor \bmod m$$

In the following analysis, it can be checked that dropping all the modulo operations, e.g.,  $\bmod m$  and  $\bmod q$ , will not change the analysis result of calculating the secret in CPAPKE.Dec, because the effect of modulo operations offsets each other. For ease of writing, we conduct the derivations without writing modulo operations. For  $\frac{q}{2^{d_v}} \cdot c_2 - \mathbf{s}^T \cdot \mathbf{u} = \lfloor \frac{q}{m} \rfloor \cdot k + (\mathbf{e} - \mathbf{e}_1)^T \cdot \mathbf{r} - \mathbf{s}^T \cdot (\mathbf{e}_1 - \mathbf{e}_2) + e_2 + \varepsilon_v$ , define  $Err = (\mathbf{e} - \mathbf{e}_1)^T \cdot \mathbf{r} - \mathbf{s}^T \cdot (\mathbf{e}_1 - \mathbf{e}_2) + e_2 + \varepsilon_v$  and  $\varepsilon' = \frac{q}{m} - \lfloor \frac{q}{m} \rfloor$  we obtain

$$\left\lfloor \frac{m}{q} \left( \frac{q}{2^{d_v}} \cdot c_2 - \mathbf{s}^T \cdot \mathbf{u} \right) \right\rfloor = \left\lfloor k + \frac{m}{q} (Err - \varepsilon' \cdot k) \right\rfloor.$$

Note that the term  $k$  is the secret encrypted in CPAPKE.Enc. To decrypt correctly in CPAPKE.Dec, the rounding  $\lfloor k + \frac{m}{q} (Err - \varepsilon' \cdot k) \rfloor$  above must equals  $k$ , which is equivalent to

$$-\frac{1}{2} \leq \left\| \frac{m}{q} (Err - \varepsilon' \cdot k) \right\|_{\infty}^{\pm} < \frac{1}{2}.$$

Equivalently, for all  $k \in \mathbb{Z}_m^n$ , we categorize the analysis into two cases. Then we have

$$\begin{cases} -\frac{q}{2m} + \varepsilon'(m-1) \leq \left\| Err \right\|_{\infty}^{\pm} < \frac{q}{2m}, \varepsilon' \geq 0 \\ -\frac{q}{2m} \leq \left\| Err \right\|_{\infty}^{\pm} < \frac{q}{2m} + \varepsilon'(m-1), \varepsilon' < 0, \end{cases}$$

$$\begin{cases} \delta = \Pr \left[ \neg \left( -\frac{q}{2m} + \varepsilon'(m-1) \leq \left\| Err \right\|_{\infty}^{\pm} < \frac{q}{2m} \right) \right], \varepsilon' \geq 0 \\ \delta = \Pr \left[ \neg \left( -\frac{q}{2m} \leq \left\| Err \right\|_{\infty}^{\pm} < \frac{q}{2m} + \varepsilon'(m-1) \right) \right], \varepsilon' < 0. \end{cases}$$

Under the assumptions of MLWE, all the coefficients of  $\mathbf{t}'$ ,  $\mathbf{u}'$  and  $v'$  follow the uniform distribution independently over  $\mathbb{Z}_q$  [4], from which the distributions of the coefficients of  $\mathbf{e}_1$ ,  $\mathbf{e}_2$  and  $\varepsilon_v$  can be computed. Moreover, the coefficients of  $\mathbf{e}$ ,  $\mathbf{r}$ ,  $\mathbf{s}$ ,  $\mathbf{e}_1$  and  $e_2$  follow some known distributions. Therefore, the distributions of the coefficients of  $Err$  can be obtained according to the distributions above. Given any parameter set, we can calculate  $\delta$  using a Python script modified from [6,3,4]. In Section 6, we calculate and present the new error probabilities of Kyber with our decryption method, where on the same parameters our decryption method is more efficient and is always less error-prone.

## 4 A Systematized Study of NTT

Traditional NTT has the following restrictions:  $2n|(q-1)$  and  $n$  be a power of two. In recent years, several variants of NTT were proposed to relax the restriction and extend the applicability of NTT. In this section, we make a deep and systematized study of NTT. First, we show the computational equivalence of Pt-NTT [29,30] and T-NTT [3]. Combining the advantages of both Pt-NTT and T-NTT, we come up with a new variant named Hybrid-NTT (H-NTT, for short). In particular, we consider the case when H-NTT reaches its optimum in computational complexity. H-NTT is used in Section 7 for the unified and compatible implementations of the KEM schemes encapsulating 512 bits.

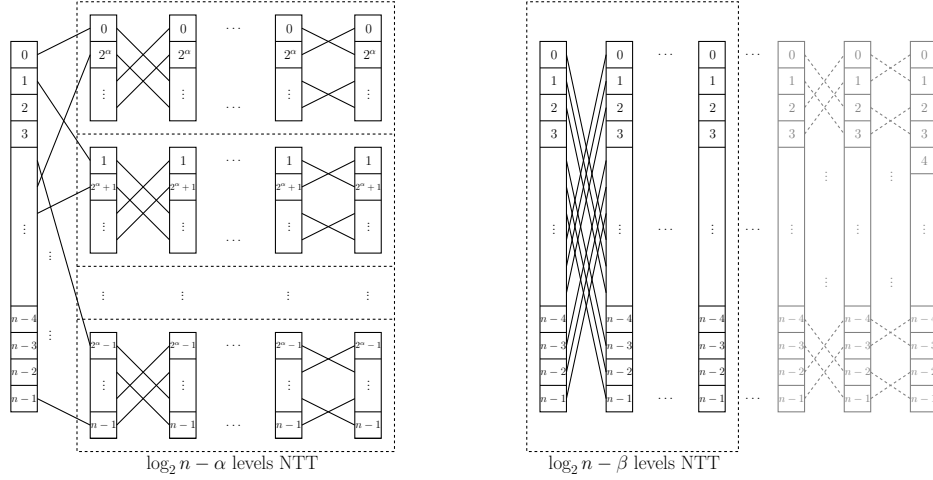


**Fig. 2.** The process of Pt-NTT and T-NTT. In Pt-NTT (left), the polynomial is split into  $2^\alpha$  sub-polynomials, and in T-NTT (right)  $\beta$  levels are cropped from the bottom.

#### 4.1 Computational Equivalence of Two Approaches

Let  $\alpha$  and  $\beta$  be nonnegative integers. Pt-NTT [29,30] follows the “upper dividing approach”, where  $\alpha$  levels of 2-division are made from the top. On the contrary, T-NTT follows the “bottom cropping” approach [1,3], where  $\beta$  levels are cropped from the bottom. These processes are shown in Figure 2. Though the two approaches appear to be quite different in nature, we show that they are actually computationally equivalent.

The analysis of the following proposition is given in Appendix A.

**Proposition 1.** *The computational complexity of multiplication and addition in generalized Pt-NTT for any  $\alpha \geq 0$  are:*

$$\begin{aligned}
 - T_m(\text{Pt-NTT}) &= \begin{cases} \frac{3}{2}n\log n + (3 \cdot 2^{\alpha-2} + \frac{3}{2} - \frac{3\alpha}{2})n, & \alpha \geq 1. \\ \frac{3}{2}n\log n + 2n, & \alpha = 0 \text{ (i.e., } \widehat{\text{NTT}}\text{).} \end{cases} \\
 - T_a(\text{Pt-NTT}) &= 3n\log n + (5 \cdot 2^{\alpha-1} - \frac{5}{2} - 3\alpha)n.
 \end{aligned}$$

**Theorem 1.** *Pt-NTT and T-NTT are computationally equivalent for any  $\alpha = \beta$ , thus the computational complexity of T-NTT can be derived from Pt-NTT, i.e.,  $T_m(\text{T-NTT}) = T_m(\text{Pt-NTT})$  and  $T_a(\text{T-NTT}) = T_m(\text{Pt-NTT})$ .*

*Proof.* First we use  $\alpha = 1$  and  $\beta = 1$  as a special case. This proof also applies to the general case. Let  $y = x^2$ . Decomposing the polynomial coefficients by parity terms, we can obtain  $f = f_e + xf_o$  and  $g = g_e + xg_o$ , i.e.,

$$\begin{cases} f_e = f_0 + f_2y + \dots + f_{n-2}y^{\frac{n}{2}-1} \\ f_o = f_1 + f_3y + \dots + f_{n-1}y^{\frac{n}{2}-1} \end{cases}, \quad \begin{cases} g_e = g_0 + g_2y + \dots + g_{n-2}y^{\frac{n}{2}-1} \\ g_o = g_1 + g_3y + \dots + g_{n-1}y^{\frac{n}{2}-1} \end{cases}$$

Then the multiplication of two polynomials can be expressed as  $h = fg = h_e + xh_o$ , where  $h_e = f_e g_e + x^2 f_o g_o$  and  $h_o = f_o g_e + f_e g_o$ .

When it comes to T-NTT, according to Definition 2 and (2), we can get the following matrix form:

$$\begin{bmatrix} \widehat{f}_0 + \widehat{f}_1 x \\ \widehat{f}_2 + \widehat{f}_3 x \\ \vdots \\ \widehat{f}_{n-2} + \widehat{f}_{n-1} x \end{bmatrix} = \mathbf{W}_{\frac{n}{2}} \begin{bmatrix} f_0 + f_1 x \\ f_2 + f_3 x \\ \vdots \\ f_{n-2} + f_{n-1} x \end{bmatrix}, \text{ i.e., } \begin{bmatrix} \widehat{f}_0 \\ \widehat{f}_2 \\ \vdots \\ \widehat{f}_{n-2} \end{bmatrix} + x \begin{bmatrix} \widehat{f}_1 \\ \widehat{f}_3 \\ \vdots \\ \widehat{f}_{n-1} \end{bmatrix} = \mathbf{W}_{\frac{n}{2}} \begin{bmatrix} f_0 \\ f_2 \\ \vdots \\ f_{n-2} \end{bmatrix} + x \mathbf{W}_{\frac{n}{2}} \begin{bmatrix} f_1 \\ f_3 \\ \vdots \\ f_{n-1} \end{bmatrix}, \text{ then}$$

we get  $\begin{bmatrix} \widehat{f}_0 \\ \widehat{f}_2 \\ \vdots \\ \widehat{f}_{n-2} \end{bmatrix} = \mathbf{W}_{\frac{n}{2}} \begin{bmatrix} f_0 \\ f_2 \\ \vdots \\ f_{n-2} \end{bmatrix} = \text{NTT}(f_e)$  and  $\begin{bmatrix} \widehat{f}_1 \\ \widehat{f}_3 \\ \vdots \\ \widehat{f}_{n-1} \end{bmatrix} = \mathbf{W}_{\frac{n}{2}} \begin{bmatrix} f_1 \\ f_3 \\ \vdots \\ f_{n-1} \end{bmatrix} = \text{NTT}(f_o)$ . Meanwhile, the pointwise multiplication in T-NTT is equivalent to

$$\begin{bmatrix} \widehat{f}_0 \\ \widehat{f}_2 \\ \vdots \\ \widehat{f}_{n-2} \end{bmatrix} \circ \begin{bmatrix} \widehat{g}_0 \\ \widehat{g}_2 \\ \vdots \\ \widehat{g}_{n-2} \end{bmatrix} + x^2 \begin{bmatrix} \widehat{f}_1 \\ \widehat{f}_3 \\ \vdots \\ \widehat{f}_{n-1} \end{bmatrix} \circ \begin{bmatrix} \widehat{g}_1 \\ \widehat{g}_3 \\ \vdots \\ \widehat{g}_{n-1} \end{bmatrix} + x \left( \begin{bmatrix} \widehat{f}_1 \\ \widehat{f}_3 \\ \vdots \\ \widehat{f}_{n-1} \end{bmatrix} \circ \begin{bmatrix} \widehat{g}_0 \\ \widehat{g}_2 \\ \vdots \\ \widehat{g}_{n-2} \end{bmatrix} \right. \\
\left. + \begin{bmatrix} \widehat{f}_0 \\ \widehat{f}_2 \\ \vdots \\ \widehat{f}_{n-2} \end{bmatrix} \circ \begin{bmatrix} \widehat{g}_1 \\ \widehat{g}_3 \\ \vdots \\ \widehat{g}_{n-1} \end{bmatrix} \right). \text{ Here, } x^2 \text{ is processed as a vector } (\omega, \omega^3, \dots, \omega^{n-1})^T \text{ in pointwise multiplication.}$$

Therefore,  $\text{T-NTT}(f) \circ \text{T-NTT}(g) = \text{NTT}(f_e) \circ \text{NTT}(g_e) + \text{NTT}(y) \circ \text{NTT}(f_o) \circ \text{NTT}(g_o) + x(\text{NTT}(f_e) \circ \text{NTT}(g_o) + \text{NTT}(f_o) \circ \text{NTT}(g_e))$ , which means Pt-NTT has the same computing process as T-NTT when  $\alpha = \beta = 1$ .

Given  $\mathbb{Z}_q[x]/(x^n + 1)$  where  $n$  is a power of 2 and  $q$  is a prime satisfying  $\frac{n}{2^{\beta-1}}|(q-1)$  for any integer  $\beta \geq 0$ , the generalized form of T-NTT( $f$ ) can be illustrated as:

$$\text{T-NTT}(f) = \mathbf{W}_{\frac{n}{2^\beta}} \begin{bmatrix} f_0 + f_1 x + \dots + f_{2^\beta-1} x^{2^\beta-1} \\ f_{2^\beta} + f_{2^\beta+1} x + \dots + f_{2^{\beta+1}-1} x^{2^\beta-1} \\ \vdots \\ f_{n-2^\beta} + f_{n+1-2^\beta} x + \dots + f_{n-1} x^{2^\beta-1} \end{bmatrix}.$$

Using the same approach, the above can be extended to the general case. Thus we complete the proof of this theorem.

## 4.2 Hybrid Number Theoretic Transform

Compared with the computational complexity of classical NTT, which is mentioned in Section 2.3, it is easy to see that Pt-NTT and T-NTT both have certain computational advantages. This motivates us to investigate whether combining these two approaches could lead to a more efficient NTT algorithm, thus bringing the introduction of hybrid-NTT (H-NTT). The goal is to calculate polynomial multiplication  $h = fg$  in a more efficient and modular way.

Denote by H-NTT( $n, \alpha, \beta$ ) the H-NTT process with  $2^\alpha$  decompositions on the top and  $\beta$ -level deletions from the bottom, as illustrated in Figure 3. In this case, the parameters need to satisfy the condition that  $\frac{n}{2^{\alpha+\beta-1}}|(q-1)$ , where  $n$  and  $q$  are defined as before. This process consists of three steps: decomposition, transformation, and combination, which are specified as below:

**Decomposition:** The original polynomials  $f$  and  $g$  are split into  $2^\alpha$  parts:  $f(x) = \sum_{i=0}^{2^\alpha-1} x^i \tilde{f}_i(x^{2^\alpha})$  and  $g(x) = \sum_{i=0}^{2^\alpha-1} x^i \tilde{g}_i(x^{2^\alpha})$ , where  $i \in \{0, \dots, 2^\alpha-1\}$ . The dimension of each sub-polynomial is bounded by  $\frac{n}{2^\alpha}$ .

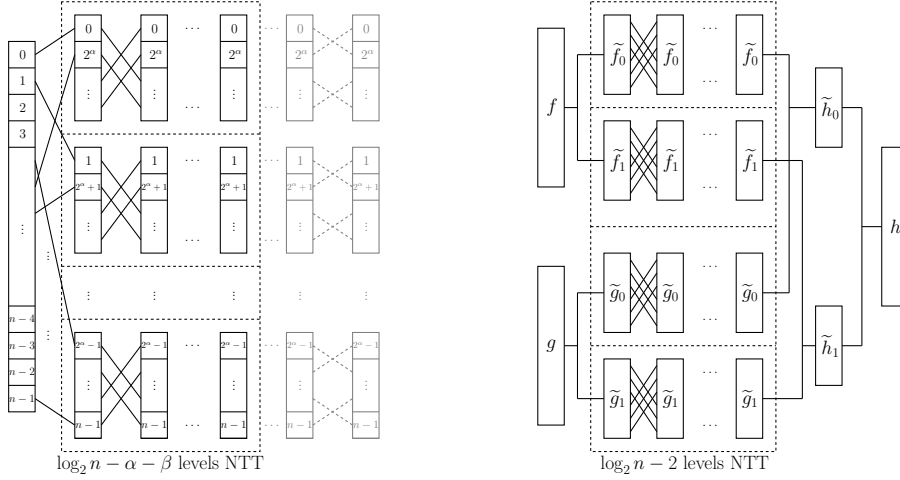


**Fig. 3.** The process of H-NTT. The polynomial is split into  $2^\alpha$  sub-polynomials, and  $\beta$  levels are omitted in transformation.

**Transformation:** The multiplication of  $f$  and  $g$  yields  $h$ , which we denote as  $h(x) = f(x)g(x) \bmod (x^n + 1) = \sum_{i=0}^{2^\alpha-1} x^i \tilde{h}_i(x^{2^\alpha})$ , where  $i \in \{0, \dots, 2^\alpha - 1\}$ . Then we have

$$\begin{aligned} \tilde{h}_i(x^{2^\alpha}) &= \sum_{l=0}^i \tilde{f}_l(x^{2^\alpha}) \tilde{g}_{i-l}(x^{2^\alpha}) + \sum_{l=i+1}^{2^\alpha-1} x^{2^\alpha} \tilde{f}_l(x^{2^\alpha}) \tilde{g}_{2^\alpha+i-l}(x^{2^\alpha}) \\ &= \text{T-NTT}^{-1} \left( \sum_{l=0}^i \text{T-NTT}(\tilde{f}_l) \circ \text{T-NTT}(\tilde{g}_{i-l}) + \sum_{l=i+1}^{2^\alpha-1} \text{T-NTT}(x^{2^\alpha}) \circ \text{T-NTT}(\tilde{f}_l) \circ \text{T-NTT}(\tilde{g}_{2^\alpha+i-l}) \right), \end{aligned}$$

where “ $\circ$ ” denotes the pointwise multiplication of polynomial vectors. Note that this definition does not affect the total number of multiplications required, which remains unchanged at  $\frac{n}{2^{\alpha+\beta}}$ . Here, we can also apply the Karatsuba technique, and then we will get  $\text{T-NTT}(\tilde{f}_i) \circ \text{T-NTT}(\tilde{g}_j) + \text{T-NTT}(\tilde{f}_j) \circ \text{T-NTT}(\tilde{g}_i) = (\text{T-NTT}(\tilde{f}_i) + \text{T-NTT}(\tilde{f}_j)) \circ (\text{T-NTT}(\tilde{g}_i) + \text{T-NTT}(\tilde{g}_j)) - \text{T-NTT}(\tilde{f}_i) \circ \text{T-NTT}(\tilde{g}_i) - \text{T-NTT}(\tilde{f}_j) \circ \text{T-NTT}(\tilde{g}_j)$ .

**Combination:**  $h(x) = \sum_{i=0}^{2^\alpha-1} x^i \tilde{h}_i(x^{2^\alpha})$ .

**Proposition 2.** *The computational complexity of multiplication and addition in H-NTT for any  $\alpha, \beta \geq 0$  is as follows:*

- $T_m(H\text{-NTT}) = \frac{3}{2}n \log n + (3 \cdot 2^{\alpha+\beta-3} + 2^{\alpha-2} + 3 \cdot 2^{\beta-3} + 2^{\alpha-\beta-2} - \frac{3}{2}(\alpha + \beta) + \frac{5}{4})n$ .
- $T_a(H\text{-NTT}) = 3n \log n + (5 \cdot 2^{\alpha+\beta-2} + 5 \cdot 2^{\beta-2} + 5 \cdot 2^{\alpha-2} - 3 \cdot (\alpha + \beta) - \frac{15}{4})n$ .

The proof of Proposition 2 is given in Appendix B. From the complexity formulas, we can derive that H-NTT reaches its optimization when  $\alpha = \beta = 1$ , where only  $\frac{3}{2}n \log n + \frac{5}{4}n$  multiplications and  $3n \log n + \frac{1}{4}n$  additions are performed. Recall that Pt-NTT (resp., T-NTT) reaches its optimization when  $\alpha = 1$  (resp.,  $\beta = 1$ ):  $\frac{3}{2}n \log n + \frac{3}{2}n$  multiplications and  $3n \log n - \frac{1}{2}n$  additions.

## 5 Expanding Key Size to 512 bits

In this section, we compare three different ways to construct KEM schemes for encapsulating 512-bit keys, and conclude with the most economic approach to this goal.

**Table 2.** Comparison of three approaches of 512-bit key

Schemes	$n$	$q$	$m$	$l$	$\eta$	$d_k$	$d_u$	$d_v$	$t_k$	$t_u$	$g$	$\delta$	$pq - sec$	$ pk $	$ ct $	$ B $
Approach 1	256	3329	2	4	2	12	11	5	0	1	$2^5$	$2^{-178.7}$	230	1568	3136	4704
Approach 2	256	7681	4	4	2	13	11	7	0	2	$2^7$	$2^{-182.9}$	208	1696	1632	3328
Approach 3	512	3329	2	2	2	12	11	5	0	1	$2^5$	$2^{-178.7}$	230	1600	1728	3328

### 5.1 Three Approaches and Comparisons

To simplify the discussion, we only focus on schemes based on Module-LWE using the compression method mentioned in section 2.5. For encapsulating a 512-bit key with at least 210-bit pq-security, there are the following three approaches:

- Approach 1: Run the KEM scheme twice, with parameters  $n = 256$ ,  $l = 4$ , and  $m = 2$ .
- Approach 2: Run the KEM scheme once, with parameters  $n = 256$ ,  $l = 4$ , and  $m = 4$ .
- Approach 3: Run the KEM scheme once, with parameters  $n = 512$ ,  $l = 2$ , and  $m = 2$ .

As described in Sections 2.5 and 3.1, let  $d_k$ ,  $d_u$ , and  $d_v$  represent the compressed length of  $\mathbf{t}$ ,  $u$ , and  $v$ . We compare these three approaches in terms of bandwidth, efficiency, error probability, compatibility, etc. The concrete analysis is as follows.

Approach 1 means the same public key is used twice in encapsulation, which will double the error probability. In this case, the bandwidth is

$$|B_1| = n + n \cdot l \cdot d_k + 2(n \cdot l \cdot d_u + n \cdot d_v) \quad (9)$$

For Approach 2, the `Encaps` function only needs to be called once, but the error probability is enlarged by the change of  $m$  from 2 to 4. With the increased value of  $m = 4$ , the other values of  $q$  and  $g$  should be doubled and the compressed length should be increased by 1 bit to avoid introducing significant decryption error. At the same time,  $\eta$  should be increased for keeping the pq-security. In this case, the bandwidth value is

$$|B_2| = n + n \cdot l \cdot (d_k + 1) + n \cdot l \cdot (d_u + 1) + n \cdot (d_v + 1) \quad (10)$$

The difference of bandwidth between Approach 1 and 2 is  $\Delta = n \cdot l \cdot (d_u - 2) + n \cdot (d_v - 1)$ . Usually  $d_u$  and  $d_v$  are not too small in practice, so  $|B_1|$  is usually much bigger than  $|B_2|$ . On the other hand, it is usually hard to consider all factors and reach a balance with Approach 2. For example, our experiments show that, though we can develop a variant of Aegis-1024 with Approach 2 where  $q = 7681$ , we failed in choosing appropriate parameters for Kyber-1024 this way for  $q = 3329$ .

For Approach 3, while  $n$  doubled, the parameter  $l$  is cut down by half. So the increase of bandwidth is reflected in two aspects: the size of `seed` and  $v$  are twice the length of before, which is actually not so significant. Our experiments show that on the same levels of security and error probability, Approach 3 leads to lower bandwidth and is more flexible in choosing parameters than Approach 2. The drawback of Approach 3 is its relatively poor modularity and compatibility in implementations. Specifically, we need to run some different NTT algorithms when implemented as the dimension now is 512 instead of 256.

With a variety of tests, we choose three parameter sets derived from Kyber-1024 in [2,3,4]. Then we instantiate the three approaches with the parameter sets, and make comparisons in Table 2. From the table we can see that, for Approach 2 in which  $q = 7681$  (as in the original Round-1 version of Kyber), if we want to keep the levels of bandwidth and error probability, the pq-security is bound to decline. By comprehensive experiments, Approach 3 achieves the balanced performance among security, bandwidth, and correctness simultaneously, and could be the best option in this scenario. As we shall show in Section 7, the problem of implementation compatibility with Approach 3 is solved with our H-NTT technique.

**Table 3.** Parameters of Kyber and OSKR

		$n$	$q$	$m$	$l$	$\eta_s$	$\eta_e$	$d_k$	$d_u$	$d_v$	$t_k$	$t_u$	$g$	$\delta$	$pq - sec$	$ pk $	$ sk $	$ ct $	$ K $	$ B $
$N = 512$	Kyber	256	3329	2	2	3	2	12	10	4	0	2	$2^4$	$2^{-138.9}$	100	800	1632	768	32	1568
	OSKR	256	3329	2	2	3	2	12	10	4	0	2	$2^4$	$2^{-142.8}$	100	800	1632	768	32	1568
$N = 768$	Kyber	256	3329	2	3	2	2	12	10	4	0	2	$2^4$	$2^{-165}$	164	1184	2400	1088	32	2272
	OSKR	256	3329	2	3	2	2	12	10	4	0	2	$2^4$	$2^{-168.8}$	164	1184	2400	1088	32	2272
$N = 1024$	Kyber	256	3329	2	4	2	2	12	11	5	0	1	$2^5$	$2^{-174.9}$	230	1568	3168	1568	32	3136
	OSKR	512	3329	2	2	2	2	12	11	5	0	1	$2^5$	$2^{-178.7}$	230	1600	3168	1728	64	3328

## 6 Applications to Kyber and Aigis

In this section, we apply the techniques proposed in this work to Kyber [4] and Aigis [28]. The resultant schemes are referred to as OSKR (standing for Optimized and Security-strengthened KybeR) and OKAI (standing for Optimized KEM from Aigis) respectively.

### 6.1 OSKR: Application to Kyber

Kyber sets  $n = 256$ ,  $q = 3329$  and  $\eta = 2$ , and provides three sets of parameters, referred to as Kyber-512, Kyber-768 and Kyber-1024 respectively, which correspond to  $l = 2, 3, 4$ . In this work, we simplify the decryption process of Kyber with the technique proposed in Section 3, and provide a new set of parameters for Kyber-1024:  $n = 512$ ,  $l = 2$  (with the same  $q = 3329$  and  $\eta = 2$ ), which is summarized in Table 3. On the same set of parameters, OSKR outperforms Kyber in faster decryption and lower error probabilities. The OSKR-1024 parameter set has doubled key size with lower error probability and the same level of security as Kyber-1024, but the bandwidth is relatively increased.

We apply our H-NTT technique with  $\alpha = \beta = 1$  to OSKR-1024. We note that the implementation of OSKR-1024 can reuse the NTT codes of Kyber/OSKR-512 (for  $n = 256$  and  $l = 2$ ) and those of Kyber/OSKR-768 (for  $n = 256$  and  $l = 3$ ). Specifically, as Kyber 512 and 768, OSKR-512 and OSKR-768 use T-NTT that is a 7-level 256-point NTT. In this work, each polynomial used in OSKR-1024 is of degree 512, and is divided into two parts of degree 256 which can then utilize the 7-level 256-point T-NTT used in Kyber-512 and Kyber-768. Our H-NTT based implementation of OSKR-1024 reuses the codes of T-NTT employed in the implementations of OSKR-512 and OSKR-768. In this sense, our H-NTT is compatible with the initial T-NTT utilized in Kyber, since the initial codes of T-NTT can be reused as a sub-procedure in H-NTT. In other words, though the parameter set is changed for OSKR-1024, there is no need for modification of codes of NTT in implementations. As a consequence, our implementation method with H-NTT can save the code size of NTT, and can improve the computational efficiency.

**On compatibility with Kyber.** OSKR-512/768 are identical to Kyber-512/768: the same parameters, the same procedures of key generation and encryption. The only difference is a faster and less error-prone decryption procedure. This means that OSKR-512/768 have remarkable compatibility with Kyber-512/1024, which do not affect the deployments of Kyber-512/768 in reality except faster and less error-prone decryption operations! The same holds for OKAI-768 and Aigis-768 that is the recommended parameter set for Aigis. If one instead insists in using Kyber-1024 for encapsulating 256-bit keys, Kyber-1024 can be optimized in the same way with our technique proposed in Section 3: faster decryption, and the error probability is lowered to  $2^{-178.7}$  from  $2^{-174.9}$  of Kyber-1024.

### 6.2 OKAI: Application to Aigis

Aigis [28] provides three sets of parameters, referred to as Aigis-512, Aigis-768 and Aigis-1024. Aigis-512 and Aigis-768 set  $(n, q) = (256, 7681)$ , while Aigis-1024 sets  $(n, q) = (512, 12289)$ . Aigis shares the same design rationales with Kyber [2,3] (specifically, the original Round-1 version of Kyber with  $q = 7681$  and both public key and ciphertext compressed), but with the following modifications: (1) Aigis-1024 encapsulates

**Table 4.** Parameters of Aigis and OKAI

		$n$	$q$	$m$	$l$	$\eta_s$	$\eta_e$	$d_k$	$d_u$	$d_v$	$t_k$	$t_u$	$g$	$\delta$	$pq - sec$	$ pk $	$ sk $	$ ct $	$ K $	$ B $
$N = 512$	Aigis	256	7681	2	2	2	12	10	9	3	3	4	$2^3$	$2^{-81.9}$	100	672	1568	672	32	1344
	OKAI	256	7681	2	2	1	4	9	8	4	4	5	$2^4$	$2^{-85.3}$	90	608	1568	640	32	1248
$N = 768$	Aigis	256	7681	2	3	1	4	9	9	4	4	4	$2^4$	$2^{-128.7}$	147	896	2208	992	32	1888
	OKAI	256	7681	2	3	1	4	9	9	4	4	4	$2^4$	$2^{-132.7}$	147	896	2208	992	32	1888
$N = 1024$	Aigis	512	12289	2	2	2	8	11	10	4	3	4	$2^4$	$2^{-211.8}$	213	1472	3392	1536	64	3008
	OKAI	512	7681	2	2	1	4	10	10	3	3	3	$2^3$	$2^{-216.2}$	208	1344	3392	1472	64	2816

512-bit key, but sets a different modulus  $q = 12289$ ; (2) Different secret and noise distributions are used for the three parameter sets of Aigis.

In this work, we present a new variant of Aigis, referred to as OKAI for simplicity: (1) We unify the parameters for all the three sets of OKAI 512, 768 and 1024, by setting the same  $q = 7681$  and the same secret and noise parameters  $\eta_s = 1$  and  $\eta_e = 4$ . This allows more compatible and unified implementations. Actually, OKAI-768 and Aigis-768 share the same set of parameters. (2) We apply the technique proposed in Section 3 to make the decryption process faster and less error-prone. The parameters for OKAI are given in Table 4. Similar to the optimization of Kyber, we apply T-NTT (with  $\beta = 1$ ) and H-NTT (with  $\alpha = \beta = 1$ ) respectively for OKAI-512/768 and OKAI-1024 respectively. Note that H-NTT for OKAI-1024 can reuse the codes of T-NTT for OKAI-512/768.

As shown in Table 4, at about the same level of security of Aigis-1024, OKAI-1024 enjoys smaller bandwidth, lower error probability, and faster decryption simultaneously. Finally, we would like to highlight some advantages of employing the unified modulus  $q = 7681$  for all the three parameter sets of OKAI:

- It allows more modular implementations, and simplifies the complexity. For example, the same modular reduction can be used for all the three cases.
- It allows more space-efficient implementations. Specifically, two pre-computed tables are needed in NTT, both of which have 128 elements when  $n = 256$ . However, the contents of the table vary with  $q$ . If  $q$  is not unified, we need more tables to store the pre-computed values of  $\zeta$ . In our implementations of OKAI, we keep  $q = 7681$  unified for both  $n = 256$  and  $n = 512$ , so the storage of these pre-computed tables, and the size of the program codes, are reduced.

## 7 Implementation and Benchmark

### 7.1 Implementation Details

**Sampling and Noise** Our parameter sets allow much faster sampling of secret and noise polynomials, because smaller size of noise requires fewer hash calls. Usually, they are sampled by centered binomial distribution  $\psi_\eta$ , which can be computed with  $\sum_{i=0}^{\eta} (a_i - b_i)$  where the bits  $a_i$  and  $b_i$  are chosen uniformly at random from  $\{0, 1\}$ . In this work, we sample them by  $\psi_2$  and  $\psi_3$  in OSKR, while  $\psi_1$  for secret and  $\psi_4$  for noise in OKAI.

**Symmetric Primitives** The symmetric primitives used to generate sufficient bytes and produce coefficients according to  $\psi$  are instantiated with functions from the FIPS-202 standard [25]. To ensure a fair comparison between different implementations, we change the SHA-2 family in Aigis and unify them into SHA-3. In detail, denote  $s$  as the *seeds*, we use the following functions:

- XOF:  $\mathcal{B}^* \times \mathcal{B} \times \mathcal{B} \rightarrow \mathcal{B}^*$  is instantiated with SHAKE-128;
- PRF( $s, b$ ):  $\mathcal{B}^{|s|} \times \mathcal{B} \rightarrow \mathcal{B}^*$  is instantiated with SHAKE-256( $s||b$ );
- KDF:  $\mathcal{B}^* \rightarrow \mathcal{B}^*$  is instantiated with SHAKE-256;
- H:  $\mathcal{B}^* \rightarrow \mathcal{B}^*$  is instantiated with SHA3-256 when  $n = 256$  and SHA3-512 when  $n = 512$ ;
- G:  $\mathcal{B}^* \rightarrow \mathcal{B}^{|s|} \times \mathcal{B}^{|s|}$  is instantiated with SHA3-512 when  $n = 256$  and SHAKE-256 with 128-bytes output when  $n = 512$ .

*Matrix Generation* Sampling the discrete Gaussian distribution is one of the most time-consuming parts of lattice-based cryptosystems [20]. In this work, we follow Kyber and Aegis and adopt the rejection-sampling method [10] to generate matrix  $\mathbf{A}$  in NTT domain. While in the case of  $n = 512$ , a few changes have been made. In detail, the *seed* has 64 bytes in length, so the loops in load, store and shuffle should be doubled. Furthermore, these optimizations do not introduce overhead in the execution time, but actually improve the efficiency to some extent as the number of hash invocations is reduced.

**Module Reduction** For Barrett reduction, the range of its input value  $a$  is  $-\frac{b}{2} \leq a < \frac{b}{2}$  where  $b = 2^{16}$  in this work, and the range of its output is  $r = a \bmod q$ . For Montgomery reduction, its input value  $a$  is a 32-bit integer ranging from  $-\frac{b}{2}q$  to  $\frac{b}{2}q$  where  $b = 2^{16}$ . The range of its output is  $-q < r < q$ . This algorithm is used to keep the product of two polynomial coefficients in the Montgomery domain. That means the product of two polynomial coefficients is still in the range of the input of Montgomery reduction. Considering this, in the process of NTT and INVNTT, the coefficients of the polynomial don't need to be reduced when  $q = 3329$ . While in the case of  $q = 7681$ , the reduction should be made every two levels. Thus, we do not need to perform modular reduction after every addition or subtraction. This lazy reduction technique allows us to reduce the number of reductions significantly.

**NTT and H-NTT** As the design rationale of H-NTT, when transforming an  $n$ -dimension polynomial to NTT domain, we split it into two  $\frac{n}{2}$ -dimension polynomials, transform them respectively, and at last combine them in the original order. However, if the coefficients are actually put in the order we need after sampling, the split and combination process can be omitted. More specifically, for a 1024-byte array which stores a 512-dimension polynomial, assuming that the  $(2i + 1)$ -th coefficients are put in the first half place and the  $2i$ -th ones are stored behind where  $i \in [0, 255]$ , then we can pass the addresses of the two half ones to the NTT function respectively. Thus, H-NTT only needs to call T-NTT twice. Considering the linear structure, the two methods are equivalent.

Then, we deal with polynomials in the form of  $a_0 + a_1x + a_2x^2 + \dots + a_{255}x^{255}$ . The T-NTT process has 7 levels in total, and there are some differences between each level when being optimized in AVX2. In level 0, the coefficient  $a_0, \dots, a_{63}$  and  $a_{128}, \dots, a_{191}$  are loaded into eight `ymm` registers. By the instructions of `vpmullw` and `vpmulhw`, the coefficients are multiplied with the first root in function `BUTTERFLY`. After that, the Montgomery reduction is needed. Then we get the result of `BUTTERFLY` by `vpaddw` and `vpsubw`. The other half of the polynomial, that is  $a_{64}, \dots, a_{127}$  and  $a_{192}, \dots, a_{255}$ , are treated in the same way. In the 1-st to 3-rd level, the coefficients are loaded directly and multiply with the relevant  $\zeta$  in `BUTTERFLY` operation. From level 4 to level 7, the coefficients need to be shuffled so the related ones can be grouped together in one register. Thus `NTTPACK` and `NTTUNPACK` functions should be called to get the right order of the polynomial.

**Karatsuba Algorithm** As we apply T-NTT and crop one level from the bottom, the pointwise multiplication should be replaced with basecase multiplication when computing the production of two polynomials: specifically, multiplying 128 linear sub-polynomials of degree 2. One common way to multiply two polynomials is to use the Schoolbook algorithm with time complexity of  $O(n^2)$ , which is applied by Kyber and Aegis [20,17,4,28]. This method needs 10 `vpmullw/vpmulhw` and 4 `vpaddw/vpaddw/vpsubd` instructions. In this work, we adopt the method of Karatsuba algorithm instead, which has time complexity  $O(n^{\log 3/\log 2})$  [16,27], with 8 `vpmullw/vpmulhw` and 8 `vpaddw/vpaddw/vpsubd` instructions. The two algorithms are shown in Table 10 and 11 in Appendix E. We achieve a slight speed acceleration after this change in the basecase multiplication. In addition, we note that for some architectures with large multiplication latency and CPI, the Karatsuba method can have more advantages over Schoolbook.

**Polynomial Compression and Serialization** The division operation in polynomial compression causes the function to consume much time, as there is no division instruction in the AVX2 instruction set. However, when replacing the division with one multiplication and one shift right operations, this function may become

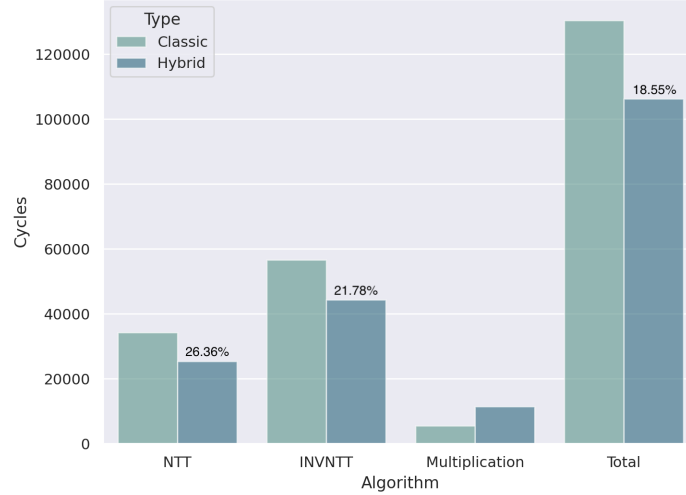


**Fig. 4.** Comparisons between classic NTT and Hybrid-NTT. We achieve 26.36% improvement in NTT, 21.78% in INVNTT, and 18.55% in the total process.

more suitable for parallel optimization. This technique has been adopted in the Round-3 submission of Kyber [4]. We note that in Aigis it remains unoptimized. Moreover, with our simplified decryption technique, the polynomial manipulation process can be further optimized.

Let  $d$  be the remaining bits after compression as before. With the increase of  $d$ , more bits are needed to store one integer in the `ymm` register. In this case, some instructions such as `vpmovzxwd` and `vpblendd` are used to pad and exchange the order of integers. And the masks should be pre-computed and stored. One thing that should be noted here is that this method may change the sequence of ciphertext. More specifically, the byte arrays are trivially serialized via the indexes in the schemes like Kyber and Aigis. However, things are different here. As we load 16 (resp., 8) coefficients to the registers each time, the polynomial coefficients are placed together at intervals of 16 (resp., 8) during serialization. Although some methods can be taken to change the positions, we think there is no need to do that because they introduce additional overhead.

**ARM Cortex-M4 Optimization** In this work we also present implementation of OSKR for ARM Cortex-M4. Our Cortex-M4 implementation is based on the `pqm4` Kyber implementation [14], and the main optimization of our work is in the processes of encryption and decryption. Specifically, we plug in the Barrett technique [5], which transforms the division into multiplication and shift right operations. Based on this, we adjust the order of the operations of (6) and (7) so that the multiplication with accumulation instruction `mla` can be used to reduce the clock cycles. Meanwhile, by using the instructions of `pkhbt` and `pkhtb`, we can pack the data and use the instruction `smuad` to reduce the computation cost further. With these modifications, we can handle each 2-bit message with 14 instructions. In the process, we also group multiple `load` and `store` operations together into consecutive instructions, because they run in 2 cycles if they are isolated but in one cycle if they follow another `load` or `store` instruction. This implementation code is presented in Algorithm 12.

## 7.2 Results and Benchmark

**Benchmark Environment** In this section, we discuss the overall impact of these proposed optimizations. Our implementations are based on and well compatible with Kyber/Aigis. All benchmarks of C and AVX2

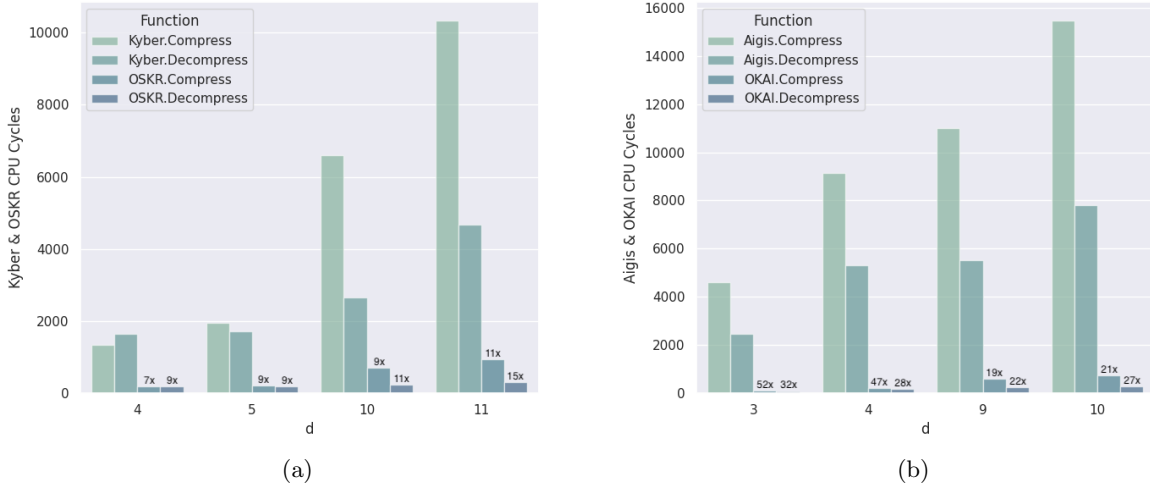


**Fig. 5.** Comparisons of polynomial compression and serialization between (a) Kyber and OSKR; (b) Aigis and OKAI. We achieve 7 $\times$  to 52 $\times$  speedup compared to the original implementations.

implementations were obtained on an Intel Core i7-9700K processor clocked at 3.6 GHz with TurboBoost and hyperthreading disabled. The benchmarking machine has 32 GB of RAM and is running macOS with version 11.0. Both implementations were compiled with Apple clang version 12.0.0.31.1. We used the compiler flags `-Wall -Wextra -Wpedantic -Wmissing-prototypes -Wredundant-decls -Wshadow -Wpointer-arith -mavx2 -mbmi2 -mpopcnt -maes -march=native -mtune=native -O0 -fomit-frame-pointer -fno-stack-check` to compile all projects. The criterion to measure algorithmic efficiency is the number of CPU cycles. All the CPU cycle counts shown are the median of the cycle counts of 10000 executions of the respective function.

For the ARM Cortex-M4 implementation, our platform is STM32F4DISCOVERY with the ARMv7E-M instruction set, which provides 196 KiB of RAM and 1 MiB of flash and runs at a maximum frequency of 168 MHz; And all the clock cycle counts shown are the median of the cycle counts of 100 executions.

We provide bar charts in this section to compare our implementations clearly with the previous works. More detailed data, including the clock cycles of each subfunction, is given in Appendix C.

**Performance of H-NTT** To compare the speed of classic NTT and H-NTT, we implement them in C with the parameters  $(n, q) = (256, 7681)$  as an example. Classic NTT does the whole 8-level NTT/INVNTT. But in H-NTT the polynomial is split into two 128-dimension sub-polynomials, where each sub-polynomial does a 6-level T-NTT/T-INVNTT with the last level cut from the bottom. The comparison results are shown in Figure 4 (Table 6). The multiplication of two polynomials needs two NTT operations, one vector multiplication, and one INVNTT operation. Although the basecase multiplication in H-NTT is slower, it is still below a tolerable level. As a whole, we show that the implementation with H-NTT is faster and speeds up the total process by 18.55%. In particular, the pre-computed constants, namely,  $\zeta$  and  $\zeta^{-1}$ , need 1024 bytes of storage in classic NTT, while in H-NTT we can reduce the storage of these constants to 256 bytes. Compared to classic-NTT, hybrid-NTT achieves both a fast speed and a significantly low storage requirement.

**AVX2 Implementation** Figure 5(a) and 5(b) (Table 7) show the speed of polynomial compression and serialization in the implementations of Kyber and Aigis (which we list as original data) and our OSKR and OKAI schemes. The cases  $d = 3, 4, 5$  are used to generate the second part of the ciphertext  $c_2$ , the others



**Fig. 6.** (a) Comparisons of Kyber, Aegis, OSKR, and OKAI in AVX2 implementations for all the three sets of parameters 512, 768 and 1024 respectively. We improve Kyber by 17%, 11% and 34%, and Aegis by 54%, 25% and 49%. (b) Comparisons of Kyber, OSKR and OKAI in ARM Cortex-M4 platform. We improve Kyber by 1%, 1% and 12%. The comparison results also show that Kyber outperforms Aegis in ARM Cortex-M4 platform

deal with  $c_1$ . In our tests, this method yields a performance speed-up between 85% and 98%, which means our method has 7 $\times$  to 52 $\times$  speedup over the original implementations.

Figure 6(a) (Table 8 and 9) reports the performance results of our implementations of OSKR and OKAI optimized using AVX2 vector instructions. As anticipated in Table 8, the performance is improved by 17.39% for Kyber-512 and 11.31% for Kyber-768. This shows the impact of our parallel polynomial manipulation. Kyber-1024 is improved by 34.26%, which embodies 37.27% in **Keypair**, 29.27% in **Encaps** and 36.74% in **Decaps**. From the analysis and experiments, we observe that the applications of our H-NTT and the new 512-bit shared key approach can bring the speed to a new level. Similarly, for Aegis, the AVX2 implementations gain up to 53.96% in performance for Aegis-512, 25.00% for Aegis-768 and 49.08% for Aegis-1024. We also record in Table 5 the size of pre-computed roots used in NTT of Aegis and in OKAI. Since  $\zeta$  changes with  $q$ , four tables for  $\zeta$  and  $\zeta^{-1}$  should be generated in Aegis. After expanding the pre-computed tables to fit the AVX2 implementations, Aegis requires 3008 bytes of storage for  $q = 7681$  and 6080 bytes for  $q = 12289$ , while OKAI only needs 1584 bytes in total. This corresponds to an 82.57% saving in memory storage. Although memory is never a constraint for C and AVX2 implementations, it is certainly worth considering in storage-limited platforms like ARM Cortex-M4.

**Table 5.** Storage size (in bytes) of the pre-computed roots for Aegis and OKAI in AVX2 implementations

	Aegis (Bytes)		OKAI (Bytes)
	$q = 7681$	$q = 12289$	$q = 7681$
$\zeta$	1504	3040	792
$\zeta^{-1}$	1504	3040	792
Total		9088	1584
Opt.			<b>82.57%</b>

**ARM Cortex-M4 Implementation** The comparisons of our ARM Cortex-M4 implementations of OSKR, OKAI and Kyber are shown in Figure 6(b) and Table 10. To the best of our knowledge, we provide the first

ARM Cortex-M4 implementation for Aegis (note that OKAI-768 and Aegis-768 are the same except a faster and less error-prone decryption process). The total cost is obtained by summing all the time spent on the three functions. Similarly, our implementation achieves the best speedup at  $N = 1024$ , with an 11.87% improvement compared with Kyber. Meanwhile, we also consider the tradeoffs between performance and memory usage. One thing should be noted is that our approaches can bring improvements with no or minimal sacrifice to memory consumption. Actually, they significantly reduce memory usage as illustrated in Table 5.

## References

1. Alkim, E., Bilgin, Y.A., Cenk, M.: Compact and simple RLWE based key encapsulation mechanism. In: LATINCRYPT 2019. vol. 11774, pp. 237–256. Springer (2019)
2. Avanzi, R., Bos, J., Ducas, L., Kiltz, E., Lepoint, T., Lyubashevsky, V., Schanck, J.M., Schwabe, P., Seiler, G., Stehlé, D.: Supporting documentation: CRYSTALS-Kyber: Algorithm Specifications And Supporting Documentation (2017), <https://csrc.nist.gov/CSRC/media/Projects/Post-Quantum-Cryptography/documents/round-1/submissions/CRYSTALS.Kyber.zip>
3. Avanzi, R., Bos, J., Ducas, L., Kiltz, E., Lepoint, T., Lyubashevsky, V., Schanck, J.M., Schwabe, P., Seiler, G., Stehlé, D.: Supporting documentation: CRYSTALS-Kyber: Algorithm Specifications And Supporting Documentation (version 2.0) (2019), <https://csrc.nist.gov/CSRC/media/Projects/Post-Quantum-Cryptography/documents/round-2/submissions/CRYSTALS-Kyber-Round2.zip>
4. Avanzi, R., Bos, J., Ducas, L., Kiltz, E., Lepoint, T., Lyubashevsky, V., Schanck, J.M., Schwabe, P., Seiler, G., Stehlé, D.: Supporting documentation: CRYSTALS-Kyber: Algorithm Specifications And Supporting Documentation (version 3.0) (2020), <https://csrc.nist.gov/CSRC/media/Projects/post-quantum-cryptography/documents/round-3/submissions/Kyber-Round3.zip>
5. Barrett, P.: Implementing the rivest shamir and adleman public key encryption algorithm on a standard digital signal processor. In: Conference on the Theory and Application of Cryptographic Techniques. pp. 311–323. Springer (1986)
6. Bos, J.W., Ducas, L., Kiltz, E., Lepoint, T., Lyubashevsky, V., Schanck, J.M., Schwabe, P., Seiler, G., Stehlé, D.: CRYSTALS - kyber: A cca-secure module-lattice-based KEM. In: EuroS&P 2018. pp. 353–367. IEEE (2018)
7. Cohen, H.: A course in computational algebraic number theory, Graduate texts in mathematics, vol. 138. Springer (1993)
8. Cook, S.A., Aanderaa, S.O.: On the minimum computation time of functions. Transactions of the American Mathematical Society **142**, 291–314 (1969)
9. Cooly, J.W., Tukey, J.W.: An algorithm for the machine calculation of complex fourier series. Mathematics of Computation. **19 (90)**, 297–301 (1965)
10. Gueron, S., Schlieker, F.: Speeding up r-lwe post-quantum key exchange. In: Nordic Conference on Secure IT Systems. pp. 187–198. Springer (2016)
11. Jaques, S., Naehrig, M., Roetteler, M., Virdia, F.: Implementing grover oracles for quantum key search on aes and lowmc. In: Annual International Conference on the Theory and Applications of Cryptographic Techniques. pp. 280–310. Springer (2020)
12. Jin, Z., Zhao, Y.: Optimal key consensus in presence of noise. arXiv preprint arXiv:1611.06150 (2016)
13. Jin, Z., Zhao, Y.: Generic and practical key establishment from lattice. In: International Conference on Applied Cryptography and Network Security. pp. 302–322. Springer (2019)
14. Kannwischer, M.J., Rijneveld, J., Schwabe, P., Stoffelen, K.: PQM4: Post-quantum crypto library for the ARM Cortex-M4
15. Karatsuba, A.A., Ofman, Y.P.: Multiplication of many-digital numbers by automatic computers. In: Doklady Akademii Nauk. vol. 145, pp. 293–294. Russian Academy of Sciences (1962)
16. Karatsuba, A.A., Ofman, Y.P.: Multiplication of many-digital numbers by automatic computers. In: Doklady Akademii Nauk. vol. 145, pp. 293–294. Russian Academy of Sciences (1962)
17. Knuth, D.E.: The art of computer programming, vol. 3. Pearson Education (1997)
18. Langlois, A., Stehlé, D.: Worst-case to average-case reductions for module lattices. Des. Codes Cryptogr. **75**(3), 565–599 (2015). <https://doi.org/10.1007/s10623-014-9938-4>
19. Lyubashevsky, V., Peikert, C., Regev, O.: On ideal lattices and learning with errors over rings. In: Annual International Conference on the Theory and Applications of Cryptographic Techniques. pp. 1–23. Springer (2010)

20. Nejatollahi, H., Dutt, N., Ray, S., Regazzoni, F., Banerjee, I., Cammarota, R.: Post-quantum lattice-based cryptography implementations: A survey. ACM Computing Surveys (CSUR) **51**(6), 1–41 (2019)
21. NIST: Post-Quantum Cryptography Standardization, <https://csrc.nist.gov/Projects/Post-Quantum-Cryptography/Post-Quantum-Cryptography-Standardization>
22. NIST: Post-Quantum Cryptography Round 3 Submissions (2020), <https://csrc.nist.gov/Projects/post-quantum-cryptography/round-3-submissions>
23. Regev, O.: On lattices, learning with errors, random linear codes, and cryptography. Journal of the ACM (JACM) **56**(6), 1–40 (2009)
24. Rescorla, E., Dierks, T.: The transport layer security (tls) protocol version 1.3 (2018)
25. of Standards, N.I., Technology: FIPS PUB 202 – SHA-3 standard: Permutation-based hash and extendable-output functions (2015), <https://nvlpubs.nist.gov/nistpubs/FIPS/NIST.FIPS.202.pdf>
26. Toom, A.L.: The complexity of a scheme of functional elements realizing the multiplication of integers. Doklady Akademii Nauk Sssr **3**(3), 496–498 (1963)
27. Weimerskirch, A., Paar, C.: Generalizations of the karatsuba algorithm for efficient implementations. IACR Cryptology ePrint Archive **2006**, 224 (2006)
28. Zhang, J., Yu, Y., Fan, S., Zhang, Z., Yang, K.: Tweaking the asymmetry of asymmetric-key cryptography on lattices: Kems and signatures of smaller sizes. In: IACR International Conference on Public-Key Cryptography. pp. 37–65. Springer (2020)
29. Zhou, S., Xue, H., Zhang, D., Wang, K., Lu, X., Li, B., He, J.: Preprocess-then-ntt technique and its applications to kyber and newhope. In: Inscrypt 2018. vol. 11449, pp. 117–137. Springer (2018)
30. Zhu, Y., Liu, Z., Pan, Y.: When NTT meets karatsuba: Preprocess-then-ntt technique revisited. IACR Cryptology ePrint Archive **2019**, 1079 (2019)

## A Proof of Proposition 1

*Proof.* The analysis of the exact computational complexity of Pt-NTT given in [29,30] is inadequate or incomplete. We make a supplementary and complete analysis on the exact computational complexity of Pt-NTT.

Let  $f(x) = \sum_{i=0}^{2^\alpha-1} x^i \tilde{f}_i(x^{2^\alpha})$  and  $g(x) = \sum_{j=0}^{2^\alpha-1} x^j \tilde{g}_j(x^{2^\alpha})$  be the decomposition of  $f$  and  $g$ . Denote  $h(x) = \sum_{k=0}^{2^\alpha-1} x^k \tilde{h}_k(x^{2^\alpha})$ , which is the multiplication of  $f(x)g(x) \bmod (x^n + 1)$ . For  $i = 0, 1, \dots, 2^\alpha - 1$ , we have

$$\begin{aligned} \tilde{h}_i(x^{2^\alpha}) &= \sum_{l=0}^i \tilde{f}_l(x^{2^\alpha}) \tilde{g}_{i-l}(x^{2^\alpha}) + \sum_{l=i+1}^{2^\alpha-1} x^{2^\alpha} \tilde{f}_l(x^{2^\alpha}) \tilde{g}_{2^\alpha+i-l}(x^{2^\alpha}) \\ &= \widehat{\text{NTT}}^{-1} \left( \sum_{l=0}^i \widehat{\text{NTT}}(\tilde{f}_l(x^{2^\alpha})) \circ \widehat{\text{NTT}}(\tilde{g}_{i-l}(x^{2^\alpha})) + \sum_{l=i+1}^{2^\alpha-1} \widehat{\text{NTT}}(x^{2^\alpha}) \circ \widehat{\text{NTT}}(\tilde{f}_l(x^{2^\alpha})) \circ \widehat{\text{NTT}}(\tilde{g}_{2^\alpha+i-l}(x^{2^\alpha})) \right). \end{aligned}$$

Meanwhile, combining with the Karatsuba technique, for any  $i \neq j$  we have  $\widehat{\text{NTT}}(\tilde{f}_i) \circ \widehat{\text{NTT}}(\tilde{g}_j) + \widehat{\text{NTT}}(\tilde{f}_j) \circ \widehat{\text{NTT}}(\tilde{g}_i) = (\widehat{\text{NTT}}(\tilde{f}_i) \circ \widehat{\text{NTT}}(\tilde{f}_j)) \circ (\widehat{\text{NTT}}(\tilde{g}_i) \circ \widehat{\text{NTT}}(\tilde{g}_j)) - \widehat{\text{NTT}}(\tilde{f}_i) \circ \widehat{\text{NTT}}(\tilde{g}_i) - \widehat{\text{NTT}}(\tilde{f}_j) \circ \widehat{\text{NTT}}(\tilde{g}_j)$ . And last we can get  $h(x) = \sum_{i=0}^{2^\alpha-1} x^i \tilde{h}_i(x^{2^\alpha})$ .

From the equation we can see that the whole process take  $2^{\alpha+1} \widehat{\text{NTT}}$ s,  $2^\alpha \widehat{\text{NTT}}^{-1}$ s,  $3 \cdot 2^{2\alpha-2} + 2^{\alpha-1}$  pointwise multiplications of vectors and  $2^{2\alpha+1} + 2^{2\alpha-1} - 5 \cdot 2^{\alpha-1}$  additions of vectors. And each operation requires:

- $\widehat{\text{NTT}}$ :  $\frac{n}{2^{\alpha+1}} \log \frac{n}{2^\alpha}$  multiplications and  $\frac{n}{2^\alpha} \log \frac{n}{2^\alpha}$  additions.
- $\widehat{\text{NTT}}^{-1}$ :  $\frac{n}{2^{\alpha+1}} \log \frac{n}{2^\alpha} + \frac{n}{2^\alpha}$  multiplications and  $\frac{n}{2^\alpha} \log \frac{n}{2^\alpha}$  additions.
- Pointwise multiplication of vectors:  $\frac{n}{2^\alpha}$  multiplications.
- Addition of vectors:  $\frac{n}{2^\alpha}$  additions.

Finally, we obtain the computational complexity of the generalized Pt-NTT with  $\alpha \geq 0$ :

- $T_m(\text{Pt-NTT}) = \begin{cases} \frac{3}{2}n \log n + (3 \cdot 2^{\alpha-2} + \frac{3}{2} - \frac{3\alpha}{2})n, & \alpha \geq 1. \\ \frac{3}{2}n \log n + 2n, & \alpha = 0 \text{ (i.e., } \widehat{\text{NTT}}\text{).} \end{cases}$
- $T_a(\text{Pt-NTT}) = 3n \log n + (5 \cdot 2^{\alpha-1} - \frac{5}{2} - 3\alpha)n.$

In comparison, the computational complexity analysis of Pt-NTT in [30] is incomplete and incorrect. For one, the complexity of addition is not analyzed in [30]. For the other, the complexity of multiplication is incorrectly asserted as  $T(n) = 3n \log n + (3 \cdot 2^{\alpha-2} - 3\alpha + \frac{1}{2})n$ .

## B Proof of Proposition 2

*Proof.* We only consider the complexity in the transformation step, which contains  $2^{\alpha+1}$  T-NTTs,  $2^\alpha$  T- $\text{NTT}^{-1}$ s,  $2^{2\alpha-1} + 2^{\alpha-1}$  pointwise multiplications of polynomial vectors,  $2^{2\alpha-2}$  pointwise multiplications of vectors, and  $2^{2\alpha+1} + 2^{2\alpha-1} - 5 \cdot 2^{\alpha-1}$  additions of polynomials, while each process requires different numbers of additions and multiplications:

- T-NTT:  $\frac{n}{2^{\alpha+1}}(\log \frac{n}{2^\alpha} - \beta)$  multiplications and  $\frac{n}{2^\alpha}(\log \frac{n}{2^\alpha} - \beta)$  additions.
- T- $\text{NTT}^{-1}$ :  $\frac{n}{2^{\alpha+1}}(\log \frac{n}{2^\alpha} - \beta)$  multiplications and  $\frac{n}{2^\alpha}(\log \frac{n}{2^\alpha} - \beta)$  additions.
- Pointwise multiplication of polynomial vectors:  $(3 \cdot 2^{(\beta-2)} + \frac{1}{2}) \cdot \frac{n}{2^\alpha}$  multiplications and  $(5 \cdot 2^{(\beta-1)} - \frac{5}{2}) \cdot \frac{n}{2^\alpha}$  additions.
- Pointwise multiplication of vectors:  $\frac{n}{2^{\alpha+\beta}}$  multiplications.
- Addition of polynomials:  $\frac{n}{2^\alpha}$  additions.

Finally, by combining all these listed above, we obtain the computational complexity of H-NTT in its generalized form.

## C CPU Cycle Counts

**Table 6.** Performance of classic-NTT and hybrid-NTT

	NTT (cycles)	INVNTT (cycles)	Multiplication (cycles)	Total (cycles)
Classic	34171	56609	5443	130394
Hybrid	25265	44280	11390	106200
<b>Speedup</b>	<b>26.36%</b>	<b>21.78%</b>	-	<b>18.55%</b>

**Table 7.** Performance of polynomial compression before and after optimization

d	Kyber vs. OSKR (cycles)					Aigis vs. OKAI (cycles)			
	4	5	10	11	3	4	9	10	
Com.	Origin	1332	1958	6600	10336	4588	9152	10988	15468
	Opt.	196	211	712	934	88	196	584	734
	<b>Speedup</b>	<b>85.3%</b>	<b>89.2%</b>	<b>89.2%</b>	<b>91.0%</b>	<b>98.1%</b>	<b>97.9%</b>	<b>94.7%</b>	<b>95.3%</b>
Decom.	Origin	1656	1722	2644	4666	2462	5298	5520	7814
	Opt.	192	199	246	306	78	192	250	294
	<b>Speedup</b>	<b>88.4%</b>	<b>88.4%</b>	<b>90.7%</b>	<b>93.4%</b>	<b>96.8%</b>	<b>96.4%</b>	<b>95.5%</b>	<b>96.2%</b>

**Table 8.** Cycle counts of Kyber and our OSKR AVX2 implementations

		Keypair (cycles)	Encaps (cycles)	Decaps (cycles)	Total (cycles)
$N = 512$	Kyber	307876	357200	321622	986698
	OSKR	262330	297228	255562	815120
	<b>Speedup</b>	<b>14.79%</b>	<b>16.79%</b>	<b>20.54%</b>	<b>17.39%</b>
$N = 768$	Kyber	501066	560478	507856	1569400
	OSKR	444730	500434	446660	1391824
	<b>Speedup</b>	<b>11.24%</b>	<b>10.71%</b>	<b>12.05%</b>	<b>11.31%</b>
$N = 1024$	Kyber	809600	895940	823304	2528844
	OSKR	507902	633722	520816	1662440
	<b>Speedup</b>	<b>37.27%</b>	<b>29.27%</b>	<b>36.74%</b>	<b>34.26%</b>

**Table 9.** Cycle counts of Aigis and our OKAI implementations

		Keypair (cycles)	Encaps (cycles)	Decaps (cycles)	Total (cycles)
$N = 512$	Aigis	654013	710023	700813	2064849
	OKAI	295014	347975	307627	950616
	<b>Speedup</b>	<b>54.89%</b>	<b>50.99%</b>	<b>56.10%</b>	<b>53.96%</b>
$N = 768$	Aigis	725454	800740	789990	2316184
	OKAI	554105	612110	570809	1737024
	<b>Speedup</b>	<b>23.62%</b>	<b>23.56%</b>	<b>27.74%</b>	<b>25.00%</b>
$N = 1024$	Aigis	1176718	1336911	1302255	3815884
	OKAI	593401	719452	630103	1942956
	<b>Speedup</b>	<b>49.57%</b>	<b>46.19%</b>	<b>51.61%</b>	<b>49.08%</b>

**Table 10.** Cycle counts of Kyber, our OSKR and OKAI ARM Cortex-M4 implementations

		Keypair (cycles)	Encaps (cycles)	Decaps (cycles)	Total (cycles)
$N = 512$	Kyber	463343	566744	525141	1555228
	OSKR	458201	565392	519635	1543228
	OKAI	513730	670337	652899	1836966
$N = 768$	Kyber	763979	923856	862176	2550011
	OSKR	748518	921330	855505	2525353
	OKAI	950675	1146910	1120283	3217868
$N = 1024$	Kyber	1216669	1406588	1326182	3949439
	OSKR	899300	1391883	1189311	3480494
	OKAI	1066979	1480010	1358412	3905401

## D Algorithm Specifics for Kyber and Aigis

---

**Algorithm 4** Kyber CPA Key Generation

---

```

1: function KYBER.CPA.KEYGEN()
2:    $\sigma, \rho \leftarrow \{0, 1\}^n$ 
3:    $\mathbf{A} \sim \mathbb{R}_q^{l \times l} := \text{Parse}(\text{Sam}(\rho))$ 
4:    $(\mathbf{s}, \mathbf{e}) \sim \psi_{\eta_s}^l \times \psi_{\eta_e}^l := \text{CBD}(\sigma)$ 
5:    $\mathbf{t} := \mathbf{A}\mathbf{s} + \mathbf{e}$ 
6:   return  $(pk := (\mathbf{t}, \rho), sk := \mathbf{s})$ 
7: end function

```

---



---

**Algorithm 5** Kyber CPA Encryption

---

```

1: function KYBER.CPA.ENC( $pk, msg, r$ )
2:    $\hat{\mathbf{A}} \sim \mathbb{R}_q^{l \times l} := \text{Parse}(\text{Sam}(\rho))$ 
3:    $(\mathbf{r}, \mathbf{e}_1, e_2) \sim \psi_{\eta_s}^l \times \psi_{\eta_e}^l \times \psi_{\eta_e}^l := \text{CBD}(r)$ 
4:    $\mathbf{u} := \hat{\mathbf{A}}^T \cdot \mathbf{r} + \mathbf{e}_1$ 
5:    $v := \mathbf{t}^T \cdot \mathbf{r} + e_2$ 
6:    $v := v + \text{Decompress}_q(msg, d_m)$ 
7:    $c_1 := \text{Compress}_q(\mathbf{u}, d_u)$ 
8:    $c_2 := \text{Compress}_q(v, d_v)$ 
9:   return  $ct := (c_1, c_2)$ 
10: end function

```

---



---

**Algorithm 6** Kyber CPA Decryption

---

```

1: function KYBER.CPA.DEC( $sk, ct$ )
2:    $\mathbf{u} := \text{Decompress}_q(c_1, d_u)$ 
3:    $v := \text{Decompress}_q(c_2, d_v)$ 
4:    $msg := \text{Compress}_q(v - \mathbf{s}^T \cdot \mathbf{u}, d_m)$ 
5:   return  $msg$ 
6: end function

```

---



---

**Algorithm 7** Aigis CPA Key Generation

---

```

1: function AIGIS.CPA.KEYGEN()
2:    $\sigma, \rho \leftarrow \{0, 1\}^n$ 
3:    $\mathbf{A} \sim \mathbb{R}_q^{l \times l} := \text{Parse}(\text{Sam}(\rho))$ 
4:    $(\mathbf{s}, \mathbf{e}) \sim \psi_{\eta_s}^l \times \psi_{\eta_e}^l := \text{CBD}(\sigma)$ 
5:    $\mathbf{t} := \text{Compress}_q(\mathbf{A}\mathbf{s} + \mathbf{e}, d_t)$ 
6:   return  $(pk := (\mathbf{t}, \rho), sk := \mathbf{s})$ 
7: end function

```

---

---

**Algorithm 8** Aigis CPA Encryption

---

```
1: function AIGIS.CPA.ENC( $pk, msg, r$ )
2:    $\hat{\mathbf{t}} := \text{Decompress}_q(\mathbf{t}, d_t)$ 
3:    $\hat{\mathbf{A}} \sim \mathbb{R}_q^{l \times l} := \text{Parse}(\text{Sam}(\rho))$ 
4:    $(\mathbf{r}, \mathbf{e}_1, e_2) \sim \psi_{\eta_s}^l \times \psi_{\eta_e}^l \times \psi_{\eta_e} := \text{CBD}(r)$ 
5:    $\mathbf{u} := \hat{\mathbf{A}}^T \cdot \mathbf{r} + \mathbf{e}_1$ 
6:    $v := \hat{\mathbf{t}}^T \cdot \mathbf{r} + e_2$ 
7:    $v := v + \text{Decompress}_q(msg, d_m)$ 
8:    $c_1 := \text{Compress}_q(\mathbf{u}, d_u)$ 
9:    $c_2 := \text{Compress}_q(v, d_v)$ 
10:  return  $ct := (c_1, c_2)$ 
11: end function
```

---

---

**Algorithm 9** Aigis CPA Decryption

---

```
1: function AIGIS.CPA.DEC( $sk, ct$ )
2:    $\mathbf{u} := \text{Decompress}_q(c_1, d_u)$ 
3:    $v := \text{Decompress}_q(c_2, d_v)$ 
4:    $msg := \text{Compress}_q(v - \mathbf{s}^T \cdot \mathbf{u}, d_m)$ 
5:   return  $msg$ 
6: end function
```

---

## E Algorithm Specifics for Polynomial Multiplication

---

**Algorithm 10** AVX2 Schooolbook Polynomial Multiplication

---

**INPUT:** Two vectorized polynomials  $a + bx$  and  $c + dx$   
**OUTPUT:**  $e + fx = ((a + bx) \cdot (c + dx)) \pmod{(x^2 \pm r)}$

```
1: vmovdqa  $\{a, b, c, d\}$  ▷ Load
2: vpmul $\{l|h\}w \{ac, ad, bc, bd\}_{\{hi,lo\}} \leftarrow \{ac, ad, bc, bd\}$  ▷ Multiplication
3: vpmul $\{l|h\}w, \text{vpsubw} \ bd' \leftarrow bd_{\{hi,lo\}}$  ▷ Reduce
4: vpmul $\{l|h\}w \ rbd_{\{hi,lo\}} \leftarrow r \cdot bd'$  ▷ Multiplication
5: vpunpck $\{l|h\}wd \ \{ac, ad, bc, rbd\} \leftarrow \{ac, ad, bc, rbd\}_{\{hi,lo\}}$  ▷ Unpack
6: vpadd, vpsubd  $\{e, f\} \leftarrow \{ac \pm rbd, ad + bc\}$  ▷ Add or sub
```

---

---

**Algorithm 11** AVX2 Karatsuba Polynomial Multiplication

---

**INPUT:** Two vectorized polynomials  $a + bx$  and  $c + dx$   
**OUTPUT:**  $e + fx = ((a + bx) \cdot (c + dx)) \pmod{(x^2 \pm r)}$

```
1: vmovdqa  $\{a, b, c, d\}$  ▷ Load
2: vpaddw  $\{t_1, t_2\} \leftarrow \{a + b, c + d\}$  ▷ Add
3: vpmul $\{l|h\}w \ \{ac, bd, m\}_{\{hi,lo\}} \leftarrow \{a \cdot c, b \cdot d, t_1 \cdot t_2\}$  ▷ Multiplication
4: vpmul $\{l|h\}w, \text{vpsubw} \ bd' \leftarrow bd_{\{hi,lo\}}$  ▷ Reduce
5: vpmul $\{l|h\}w \ rbd_{\{hi,lo\}} \leftarrow r \cdot bd'$  ▷ Multiplication
6: vpunpck $\{l|h\}wd \ \{ac, bd, rbd, m\} \leftarrow \{ac, bd, rbd, m\}_{\{hi,lo\}}$  ▷ Unpack
7: vpadd  $n \leftarrow ac + bd$  ▷ Add
8: vpadd, vpsubd  $\{e, f\} \leftarrow \{ac \pm rbd, m - n\}$  ▷ Add or sub
```

---

---

**Algorithm 12** Optimized Enc/Dec on ARM Cortex-M4

---

**INPUT:** Message  $m$  to be encrypted and polynomial  $s$

**OUTPUT:** Compressed ciphertext  $c_2$

```
1: lsr  polyk, m, shiftbits
2: bfi  polyk, polyk, #15, #2
3: and  polyk, #0X00010001
4: pkhbt pack, polyk, stmp0, lsl#16
5: smuad pack, pack, mult
6: mla  pack, pack, magic, ad
7: lsr  pack, pack, #26
8: and  result1, pack, #15
9: pkhtb pack, stmp0, polyk, asr#16
10: smuad pack, pack, mult
11: mla  pack, pack, magic, ad
12: lsr  pack, pack, #22
13: and  pack, pack, #0Xf0
14: orr  result1, result1, pack
```

---